

A NOVEL POST-TRANSLATIONAL MODIFICATION ON THE CENTRAL CRISPR
ENZYME: DISCOVERY OF CAS9 UBIQUITYLATION

by

Arda Baran Çelen

B.S., Biological Sciences, Florida State University, 2015

Submitted to the Institute for Graduate Studies in
Science and Engineering in partial fulfillment of
the requirements for the degree of
Master of Science

Graduate Program in Molecular Biology and Genetics
Boğaziçi University
2019

ACKNOWLEDGEMENTS

ABSTRACT

A NOVEL POST-TRANSLATIONAL MODIFICATION ON THE CENTRAL CRISPR ENZYME: DISCOVERY OF CAS9 UBIQUITYLATION

The CRISPR/Cas9 system offers a simple method for genome engineering by utilizing the ability of the bacterial Cas9 enzyme to cleave any desired genomic region under the guidance of a complementary RNA molecule. Due to its minimalism and versatility, the CRISPR/Cas9 system is increasingly being used as a gene editing platform in higher organisms, with the current applications encompassing diverse fields such as disease therapy, biotechnology and agriculture. Despite such widespread use of this prokaryotic protein, there is a lack of knowledge regarding its behavior and regulation in eukaryotic systems where the majority of these applications are implemented.

In this study, we aim to elucidate the mechanisms of Cas9 regulation in eukaryotic systems with the specific goal of investigating the potential post-translational modifications (PTMs) on this protein. As part of this, we show that Cas9 gets ubiquitylated, promoting its proteasomal degradation. In addition, we present a cell culture-based experimental setup where we aim to discover that the *Streptococcus pyogenes* Cas9 protein undergoes SUMO modification following the engulfment of these bacteria by human immune cells.

We expect that these results will lead to a better understanding of the eukaryotic post-translational regulation of Cas9. Our hope is that uncovering the functional implications of these PTMs will contribute to the development of safer therapies and improve the current CRISPR-based applications, while paving the way for new ones. Moreover, we hope that a potential discovery of *in vivo* Cas9 sumoylation may create a new frontier for future research focusing on host-pathogen interactions.

ÖZET

CRISPR SİSTEMİNİN KİLİT ENZİMİ ÜZERİNDE YENİ BİR POSTTRANSLASYONEL MODİFİKASYON: CAS9 UBİKİTİNASYONUNUN KEŞFİ

CRISPR/Cas9 sistemi, bakteriyel Cas9 enziminin genomda arzu edilen bölgeleri tamamlayıcı bir RNA molekülünün yönlendirmesi neticesinde keşilmesi özelliğini kullanan bir genom mühendisliği metodudur. Bu sistem, minimalist ve uyarlanabilir gen editleme platformu olması sebebiyle gelişmiş organizmalarda gittikçe daha yaygın bir biçimde kullanılmaktadır. Sistemin günümüzdeki uygulamaları hastalık terapisi, biyoteknoloji ve ziraat gibi farklı alanları kapsar. Bu prokaryotik proteinin kullanımının bu denli yaygın olmasına rağmen, uygulamaların en yaygın olduğu ökaryotik sistemlerde nasıl davrandığına ve regüle edildiğine dair fazla bilgimiz yoktur.

Bu çalışmada, Cas9'un ökaryotik sistemlerde nasıl regüle edildiğini, uğradığı potansiyel post translasyonel modifikasyonlar (PTM'ler) bağlamında inceleyerek ortaya çıkarmayı amaçlamaktayız. Bu hedefin bir parçası olarak Cas9'un ubikitin modifikasyonuna ve neticesinde proteazomal yıkılıma uğradığını gösteriyoruz. Bunun yanında, bu çalışmada insan bağışıklık sistemi hücrelerinin *Streptococcus pyogenes* bakterisini içine almasını takiben, bakterideki Cas9 proteininin hücre tarafından SUMO modifikasyonuna uğradığını gözlemlemeyi amaçladığımız bir hücre kültürü bazlı deney kurulumu sunuyoruz.

Elde ettiğimiz sonuçların, Cas9'un ökaryotik sistemlerdeki post-translasyonel modifikasyonlarının daha iyi anlaşılmasına yol açacağını düşünmekteyiz. Ümidimiz, bu PTM'lerin fonksiyonel neticelerinin ortaya çıkarılmasının, daha güvenli terapilerin geliştirilmesine ve halihazırda kullanılan CRISPR bazlı uygulamaları iyileştirilmesine katkıda bulunması ve yeni uygulamaların önünü açmasıdır. Bunun yanı sıra, Cas9'un doğada SUMO modifikasyonuna uğradığına dair olası bir keşfin, gelecekte konak-patojen etkileşimlerini inceleyecek araştırmalar için yeni bir cephe açacağını ummaktayız.

TABLE OF CONTENTS

ACKNOWLEDGEMENTS	iii
ABSTRACT	iv
ÖZET	v
LIST OF FIGURES	viii
LIST OF TABLES	x
LIST OF SYMBOLS.....	xi
LIST OF ACRONYMS / ABBREVIATIONS	xii
1. INTRODUCTION.....	1
1.1. Gene Therapy	1
1.2. Genome Editing.....	4
1.3. Discovery and Mechanism of the CRISPR/Cas System	5
1.4. Cas9: The Key Enzyme of the Type II CRISPR/Cas System	6
1.5. Structure of Cas9	7
1.6. Applications of the CRISPR/Cas9 System.....	8
1.7. Practical and Potential Issues of the CRISPR/Cas9 System	11
1.8. Posttranslational Regulation of Cas9.....	14
1.9. Ubiquitylation.....	15
1.10. Sumoylation.....	17
3. AIM OF STUDY	20
4. MATERIALS	21
4.1. Biological Materials	21
4.2. Experimental Equipments and Devices.....	21
4.3. Cell and Bacterial Culture	24
4.4. Plasmids.....	24
4.5. General Kits, Enzymes and Chemicals	25
4.6. Buffers and Antibodies.....	27
5. METHODS.....	31
5.1. Cell Culture	31

5.2. Generation of Stable Cell Lines	31
5.3. Transfection.....	32
5.4. Histidine Pulldown Assay	32
5.5. Immunoprecipitation Assay.....	34
5.6. Western Blotting.....	35
5.7. Mass Spectrometry	36
5.8. Bacterial Culture and Infection	36
5.9. Immunofluorescence	37
5.10. Proximity Ligation Assay.....	38
6. RESULTS.....	40
6.1. Generation of the Cas9-Stable HEK293 Cells	40
6.2. Investigation of Cas9 Ubiquitylation by His Pulldown Assays	41
6.3. Investigation of Cas9 Ubiquitylation by Immunoprecipitation Assay	42
6.4. Investigation of Cas9 Ubiquitylation by Proximity Ligation Assay	43
6.5. Mass Spectrometry to Determine the Ubiquitylation Sites on Cas9	45
6.6. Stability of the Ubiquitylated Cas9 Protein.....	47
6.7. Infection of Human Cell lines with <i>S. pyogenes</i>	49
7. DISCUSSION	55
7.1. Ubiquitylation of Cas9	55
7.2. Sumoylation of Cas9 in the Infection System	56
REFERENCES	59

LIST OF FIGURES

Figure 1.1. Schematic Representation of Cas/CRISPR System in Bacteria.....	6
Figure 1.2. Structural models of <i>S. pyogenes</i> and <i>S. aureus</i> Cas9 in their holo forms	8
Figure 1.3. Enzymatic machinery and functional outcomes of ubiquitylation.....	16
Figure 1.4. Structural comparison of modifier peptides and the SUMO machinery.....	17
Figure 6.1. Inducible FLAG-Cas9 expression in HEK293 cells	40
Figure 6.2. His pulldown with immunoblotting for anti-FLAG.....	41
Figure 6.3. His pulldown in Cas9-stable HEK293 cells	42
Figure 6.4. Immunoprecipitation of FLAG-Cas9 with immunoblotting for His.....	43
Figure 6.5. PLA showing interaction between Cas9 and endogenous ubiquitin.....	45
Figure 6.6. Mass Spectrometry Results Showing Ubiquitin-Modified Residues on Cas9..	47
Figure 6.7. Cycloheximide chase assay to analyze Cas9 stability.	48
Figure 6.8. Consensus sumoylation motifs on SpCas9	50
Figure 6.9. DAPI staining of HeLa cells	51

Figure 6.10. SUMO-1 and Cas9 labeling in non-infected and infected THP-1 cells.....	52
Figure 6.11. SUMO-2 labeling in THP-1 cells.....	53
Figure 6.12. Proximity ligation assay for SUMO-1-Cas9 interaction.....	54

LIST OF TABLES

Table 4.1. Equipments and Devices	21
Table 4.2. Disposable Materials	23
Table 4.3. Growth Media and Reagents	24
Table 4.4. Plasmids.....	25
Table 4.5. Kits and Reagents	25
Table 4.6. Chemicals	26
Table 4.7. Solutions and Buffers	27
Table 4.8. Antibodies	30
Table 5.1. Transfection and Treatment Plan for Histidine Pulldown.....	33
Table 6.1. Ubiquitin-Modified Cas9 Residues as Determined by Mass Spectrometry.....	46

LIST OF SYMBOLS

bp	Base pairs
cm ²	Square centimeter
g	Gram
g	Gravity
h	Hour
M	Molar
mg	Milligram
ml	Milliliter
mM	Millimolar
mm	Millimeter
ng	Nanogram
V	Volt
β	Beta
μ g	Microgram
μ l	Microliter
μ M	Micromolar
$^{\circ}$ C	Degree Celsius

LIST OF ACRONYMS / ABBREVIATIONS

ADA-SCID	Adenosine deaminase deficiency presenting with severe combined immunodeficiency
APC	Anaphase-promoting complex
APS	Ammonium persulfate
ATP	Adenosine triphosphate
BSA	Bovine serum albumin
Cas	CRISPR-associated endonuclease
CRISPR	Clustered regularly interspaced short palindromic repeats
CRISPRi	CRISPR-interference
crRNA	CRISPR RNA
DAPI	4'-6-diamidino-2-phenylindole
dCas9	dead Cas9
ddH ₂ O	Double-distilled water
DMEM	Dulbecco's modified eagle medium
DMSO	Dimethyl sulfoxide
DNA	Deoxyribonucleic acid
Dox	Doxycycline
DSB	Double-strand break
DUB	Deubiquitinase
EDTA	Ethylenediaminetetraacetic acid
EMBL	European Molecular Biology Laboratory
FBS	Fetal bovine serum
FDA	Food and Drug Administration
HBS	HEPES buffered saline solution
HDR	Homology-directed repair
His	Histidine
HEPES	4-(2-hydroxyethyl)-1-piperazineethanesulfonic acid
IP	Immunoprecipitation
iPSC	Induced pluripotent stem cell
LB	Luria-Bertani broth
Lys	Lysine

NEM	N-ethylmaleimide
NF- κ B	Nuclear factor kappa B
NFAT	Nuclear factor of activated T cells
NHEJ	Nonhomologous end-joining
OD	Optical density
OTC	Ornithine transcarbamylase
PAGE	Polyacrylamide gel electrophoresis
PAM	Protospacer-adjacent motif
PBS	Phosphate buffered saline
PBS-T	Phosphate buffered saline with Tween 20
PCNA	Proliferating cell nuclear antigen
PD	Pulldown
PFA	Paraformaldehyde
PI	Pam-interacting domain
PLA	Proximity ligation assay
PMA	Phorbol 12-myristate 13- acetate
PML	Promyelocytic leukemia protein
Pre-crRNA	Precursor CRISPR RNA
PTM	Posttranslational modification
Pup	Prokaryotic ubiquitin-like protein
RIPA	Radioimmunoprecipitation buffer
RNA	Ribonucleic acid
RNAi	RNA interference
<i>S. pyogenes</i>	<i>Streptococcus pyogenes</i>
SaCas9	<i>Staphylococcus aureus</i> Cas9
SCID-X1	X-linked severe combined immunodeficiency
SDS	Sodium dodecyl sulfate
sgRNA	Single guide RNA
SILAC	Stable isotope labeling by amino acids in cell culture
SpCas9	<i>Streptococcus pyogenes</i> Cas9
SUMO	Small ubiquitin-like modifier
TALEN	Transcription-activator-like effector nucleases
TEMED	Tetramethylethylenediamine
THB	Todd Hewitt broth

tracrRNA	<i>Trans</i> -activating CRISPR RNA
Ub	Ubiquitin
WB	Western blot
WCL	Whole cell lysate
WED	Wedge domain
ZFN	Zinc-finger nuclease

1. INTRODUCTION

Voltaire once said that the art of medicine consists of amusing the patients while nature cures the disease. As the quote illustrates, for thousands of years, the predominant attitude towards disease was one of helplessness, often infused with a sense of paranormal terror. Disease could claim anyone, anytime, ravage entire communities at once, and disappear in an instant just as it came to be. Therefore, to those born before modern medicine, this seemingly whimsical and omnipotent force was inevitably attributed to acts of supernatural beings. The shaman-doctors of the antiquity haggled with the deities to restore the afflicted to good health, the Greeks believed that sickness was a form of divine vengeance against humans for accepting the gift of fire from Prometheus, and the Middle Age Europeans banished the leprous into isolated colonies to suffer the consequence of their sins.

This pervasive pattern of desperation was punctured by the advent of the Germ Theory in the 19th century. By appreciating the connection between pathogens and disease, the science of medicine experienced a quantum leap that marked the transition into the modern era, where the use of sanitation and antimicrobial agents form a cornerstone in our efforts to fight disease. In parallel to our efforts to control infections, we discovered other environmental factors that contribute to diseases, such as bad nutrition, consumption of tobacco, and a sedentary lifestyle. However, as we peeled away at these external threats against our existence, we discovered another layer at the core, one that is much more fundamental to our being, one that consists of the blueprints to who we are. The burgeoning field of genetics in the 20th century showed us how disease and death are built into our nature, and faced with genetic diseases, humans experienced a new degree of helplessness that reduced our disease-fighting efforts to a mere attempt to manage symptoms.

1.1. Gene Therapy

Today, we are experiencing another quantum leap in medical science, thanks to the concept of gene therapy. Gene therapy revolves around the notion of expressing exogenous

DNA in the human genome in order to treat inherited diseases by compensating for the defective endogenous copy. This idea, the realization of which would enable scientists to access and manipulate our genetic codes to cure diseases, was initially conceptualized in a 1966 paper by Edward Tatum. Dr. Tatum expounded on the possibility of using viruses as vectors to deliver desired DNA molecules to a patient's isolated and cultured cells, which would then be re-implanted into the patient (Tatum, 1966). At the time, the ability of viruses to transfer genetic material between their bacterial hosts had been known for more than a decade, thanks to the careful work by Zinder and Lederberg on *Salmonella typhimurium* and its infecting phage (Zinder and Lederberg, 1952).

Two years after Edward Tatum's seminal paper, in a proof-of-concept demonstration, Rogers et al. artificially polyadenylated the tobacco mosaic virus genome in the laboratory and infected tobacco plants with this modified strain, after which they were able to isolate the corresponding poly-lysine oligopeptides from the plants (Rogers and Pfuderer, 1968). These results affirmed the theoretical suitability of viral vectors for delivering genetic material into the eukaryotic genome for expression.

The development of recombinant DNA technology in the 1970s enabled scientists to isolate and join together separate genomic fragments. For gene therapy efforts, this meant that the introduction of desired human genes into precise sites within viral genomes to be delivered into patients was now a plausible prospect. In 1990, the first FDA-approved human gene-therapy trial was initiated at the NIH Clinical Center in Maryland, with the aim of treating two children with adenosine deaminase deficiency presenting with severe combined immunodeficiency (ADA-SCID) (Blaese et al., 1995). This monogenic disorder results from a defect in the enzyme adenosine deaminase which regulates nucleic acid turnover and breaks down adenosine obtained from food (Cristalli et al., 2001). As part of this trial, the investigators used a disabled retroviral vector to transduce an intact adenosine deaminase gene into the patients' isolated peripheral blood lymphocytes, which were then transfused back to the patients. The trial results fell short of expectations, failing to demonstrate a permanent therapeutic response (Blaese et al., 1995).

Despite the initial failures, gene therapy continued to garner increased attention due to its immense potential until the death of Jesse Gelsinger in 1999 as a direct consequence

of the therapy protocols. The 18-year-old was participating in a clinical trial at the University of Pennsylvania with the hopes of overcoming a partial ornithine transcarbamylase (OTC) deficiency. During the course of the treatment, he developed a severe immune reaction to the adenoviral vector carrying the corrective gene, leading to multiple organ failure and death (Stolberg, 1999). The case brought the risks of gene therapy into public attention, and the ensuing ethical and safety concerns checked the enthusiasm of scientists who had been enthralled by the therapeutic possibilities.

Compounding the issue of immunogenicity was the possibility of insertional mutagenesis resulting from the random integration of the transgene into actively transcribed loci within the human genome. A disruption of an anti-oncogene or an upregulation of a proto-oncogene due to insertional mutagenesis can induce cancer (Baum, 2007). This hypothetical scenario became a reality during the follow-up of a gene-therapy clinical trial for X-linked severe combined immunodeficiency (SCID-X1). Despite the treatment resulting in a definitive cure for the condition (Cavazzana-Calvo et al., 2000), two of the patients developed leukemias after several years due to retroviral insertion near the promoter of a proto-oncogene called LMO2, leading to its abnormal activation (Hacein-Bey-Abina et al., 2003). As such, prevention of random integration of constructs through precise localization to specific genomic loci has become a major goal for the efforts to increase the safety and availability of this therapeutic modality. Part of these efforts has been to engineer different vectors to modify the level and duration of transgene expression in response to the given specific therapeutic context, and there has also been an increased tendency towards using lentiviral vectors which are less prone to trigger proto-oncogene activation compared to their retroviral counterparts (Lundstrom, 2018). Thanks to the increasingly safe applications of these disarmed viruses, scientists have been able to achieve impressive clinical benefits by programming T cells to express specially-engineered chimeric antigen receptor constructs that are capable of targeting lymphoid tumors (Dunbar et al., 2018). As a result of these exciting developments in the realm of gene therapy, many recent clinical trials demonstrated promising outcomes in terms of safety and efficacy for a great variety of inheritable diseases including B-cell malignancies, hemoglobinopathies, neuromuscular diseases and thalassemia (Naldini, 2015).

1.2. Genome Editing

In parallel to the development of viral vector-based gene therapy protocols, a new therapeutic modality emerged in the 21st century with the promise of reducing the risk of immunogenicity, achieving better target locus specificity and thereby entirely eliminating the issue of genotoxicity due to insertional mutagenesis. “Genome editing” sets out to resolve these problems by directly ablating or replacing the defective gene rather than merely inserting its correct copy into an unrelated locus within the genome. Moreover, whereas traditional gene therapies fail to address dominant negative mutations that result in deleterious gain-of-function phenotypes, as the supplementation of the correct gene does not eliminate the mutant copy, genome editing is able to overcome this limitation thanks to this direct targeting (Pelletier et al., 2006; Li et al., 2018). In this sense, genome editing is similar to the RNA-interference- or RNAi-based therapies which seek to silence or destroy the mutant messenger RNA products before they can be translated (Mansoori et al., 2014). However, unlike RNAi, it tackles the problem at its genetic root and thus offers a permanent solution (Li et al., 2018).

“Genome editing” refers to an array of technologies that exploit the ability of several cellular nucleases to recognize specific genomic loci and induce precise double-strand breaks (DSBs) in the DNA, with the aim of removing deleterious mutations through the activation of endogenous repair pathways (Guha et al., 2017). While the nonhomologous end-joining (NHEJ) pathway disrupts the target gene by stochastically inducing insertion or deletion mutations (indels) at the breakage site (Jeggo, 1998), homology-directed repair (HDR) can create more specific alterations by incorporating the sequence of a donor DNA template (Ahmad et al., 2018). From a therapeutic perspective, this means that HDR permits in-situ repair of pathogenic mutations through the provision of an exogenous DNA molecule carrying the “correct” nucleotide sequence (Jasin, 1996). Unfortunately, the error-prone NHEJ typically occurs more efficiently compared to HDR (Jeggo, 1998; Mao et al., 2008), and therefore, a major research focus has been finding ways to prompt the cell towards the HDR pathway in response to DSBs.

Another barrier in the way of efficient use of genome editing was the question of how to focus on a specific genomic locus to introduce a DSB, which was overcome through

the use of zinc-finger nucleases (ZFNs) and transcription-activator-like effector nucleases (TALENs) (Bibikova et al., 2002; Li et al., 2011). These nucleases can be custom-designed to bind to any desired DNA sequence with a relatively high specificity (Carroll, 2008); however, as a fundamental limitation, a given ZFN or TALEN cannot be repurposed to bind to a novel locus, as target specificity arises from these proteins' individualized amino acid sequences within their DNA binding domains (Urnov et al., 2010; Li et al., 2011; Miller et al., 2011). Therefore, each time a new DNA sequence is to be targeted for cleavage, de novo design and validation are required, impeding flexible and high-throughput application (Doudna and Charpentier, 2014; Wang et al., 2016).

1.3. Discovery and Mechanism of the CRISPR/Cas System

Arguably the greatest breakthrough in the field of genome editing was attained with the discovery and manipulation of the CRISPR (clustered regularly interspaced short palindromic repeats)/Cas (CRISPR-associated protein) system (Hsu *et al.*, 2014; Wang *et al.*, 2016). CRISPRs are short repetitive elements intercalated with unique spacer sequences within the prokaryotic genome, as first reported by Yoshizumi Ishino in *Escherichia coli* (Ishino *et al.*, 1987). Following this serendipitous discovery, numerous theoretical functions were attributed to these repetitive sequences, until a systematic analysis revealed that the spacer sequences contained within the CRISPRs matched to viral and plasmid genomic elements (Bolotin *et al.*, 2005; Mojica *et al.*, 2005; Pourcel *et al.*, 2005). In addition, several well-conserved genes were discovered to reside in the vicinity of CRISPRs in various bacteria whose protein products contained helicase- and nuclease-like domains (Jansen *et al.*, 2002; Bolotin *et al.*, 2005). The finding of the extrachromosomal origin of CRISPR loci in combination with the putative nuclease genes (named CRISPR-associated, or *cas*) gave rise to the more concrete and currently accepted model. According to this, CRISPR/Cas is a prokaryotic defense system that endows acquired immunity against foreign genetic elements such as bacteriophages and plasmids (Barrangou *et al.*, 2007) (Figure 1.1). These elements get incorporated into the CRISPR loci to confer immunological memory to the host cell. The CRISPR array, including the spacer (the incorporated protospacer), then gets transcribed to produce a precursor CRISPR RNA (pre-crRNA), which undergoes processing by Cas nucleases and other host enzymes to generate mature crRNAs (Brouns *et al.*, 2008). After this step, the mature crRNAs form a complex with the Cas nucleases and, through Watson-

Crick base pairing, guide them to recognize complementary invading genetic elements for cleavage and neutralization (Garneau *et al.*, 2010). Although the specifics vary between the six different types of CRISPR/Cas systems (I-VI) found in prokaryotes, this overall theme holds.

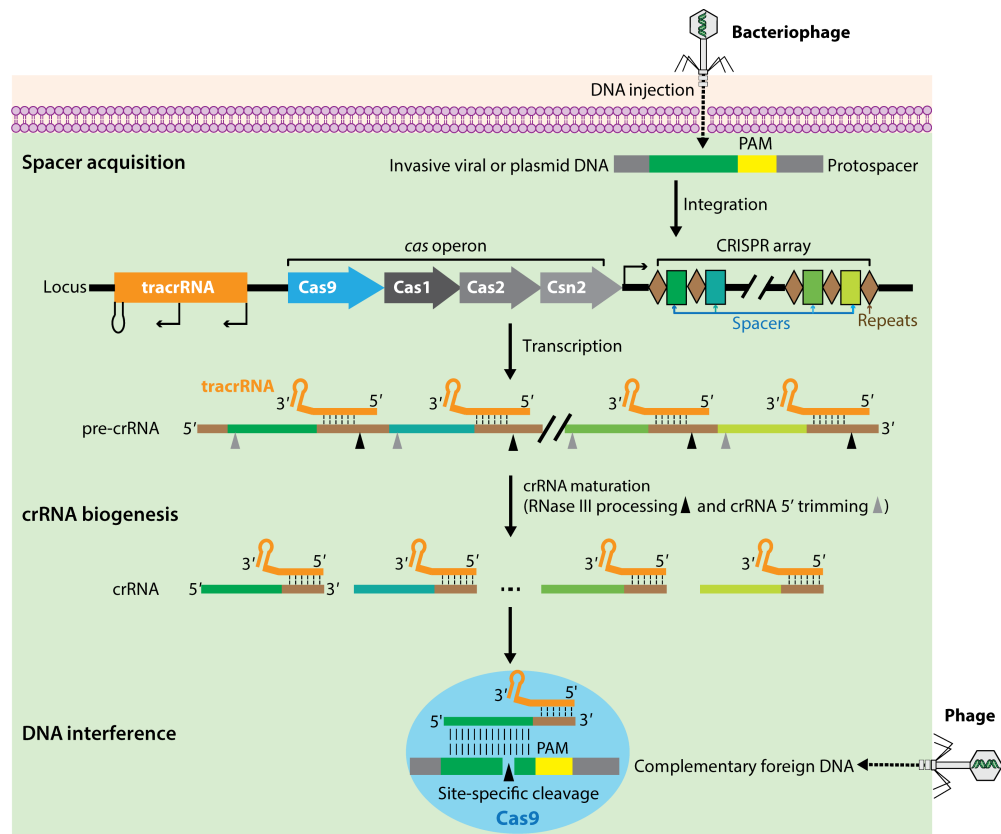


Figure 1.1. Schematic Representation of Cas/CRISPR System in Bacteria. The invading genomic element is incorporated into the bacterial genome and gives rise to crRNAs, which help the nuclease to recognize and destroy the complementary viral DNA in future infections.

1.4. Cas9: The Key Enzyme of the Type II CRISPR/Cas System

The ability of the CRISPR/Cas system to introduce DSBs in the invading genome led to the insight that the same mechanism could be exploited for host-independent genome

engineering applications (Cong *et al.*, 2013; Mali *et al.*, 2013). This was helped by the modularity of the system, in that the target specificity is mainly determined by the independently-provided guide RNA rather than the nuclease structure itself as is the case for ZFNs and TALENs (Jinek *et al.*, 2012). Moreover, the type II CRISPR/Cas system was discovered to require only a single multidomain endonuclease called Cas9 to cleave its targets, unlike the other two types that were known at the time (I and III) that rely on the coordinated activity of a multisubunit complex (Makarova *et al.*, 2015; Makarova *et al.*, 2017). More detailed studies revealed that the presence of a short (2-5 bp) protospacer-adjacent motif (PAM) flanking the 3' end of the target DNA is essential for Cas9 compatibility and also contributes to target specificity (Deveau *et al.*, 2008). This PAM is absent in the flanking regions of the host CRISPR spacer elements, and therefore the issue of self-targeting is circumvented (Leenay *et al.*, 2016).

Although the PAM requirement seems to limit the targeting scope, the particular Cas9 homologue in *Streptococcus pyogenes* (SpCas9) recognizes a relatively ubiquitous motif consisting of 5'-NGG-3', which helped it become the most popular homologue for genome editing applications (Jinek *et al.*, 2012). The type II CRISPR endonuclease homologues, including SpCas9, form their effector complexes using an additional unique RNA molecule called the *trans*-activating crRNA (tracrRNA) (Deltcheva *et al.*, 2011). While the crRNA strand hybridizes with the target DNA along a 20-bp stretch, the tracrRNA binds the crRNA, forming the functional duplex (Gasiunas *et al.*, 2012; Jinek *et al.*, 2012). This system was further simplified for laboratory applications when Martin Jinek *et al.* demonstrated that a ~100-nucleotide chimeric single guide RNA (sgRNA) engineered to contain both of these components could induce sequence-specific DSBs with comparable efficiency (Jinek *et al.*, 2012). Following these developments, the current most commonly-used system based on a single nuclease and a single guide RNA was established, and CRISPR/Cas9 became a versatile gene-targeting platform.

1.5. Structure of Cas9

The crystal structures of the *Streptococcus pyogenes*, *Staphylococcus aureus* and *Actinomyces naeslundii* Cas9 enzymes have been determined by different groups, and SpCas9 was resolved in its apo form as well as the two holo forms (bound to sgRNA or

sgRNA-DNA) (Anders *et al.*, 2014; Jiang *et al.*, 2015; Jinek *et al.*, 2014; Nishimasu *et al.*, 2014, Nishimasu *et al.*, 2015). The overall architecture of Cas9 is constituted of two lobes possessing distinctive functions, with the REC lobe being responsible for helical recognition and the NUC lobe effecting the enzyme's nuclease activity (Figure 1.2). The guide RNA-target DNA complex sits within the groove between these lobes. Comprising the NUC lobe are two separate nuclease domains called RuvC and HNH, each cleaving a separate strand within the target duplex, as well as a wedge domain (WED) and a PAM-interacting (PI) domain. Detailed understanding of these structural components led to the creation of a working model for Cas9 activation, according to which the initially autoinhibited protein becomes activated upon sgRNA binding, as the ensuing conformational change exposes the catalytic site of the HNH domain and enables DNA binding (Jinek *et al.*, 2014; Jiang *et al.*, 2015).

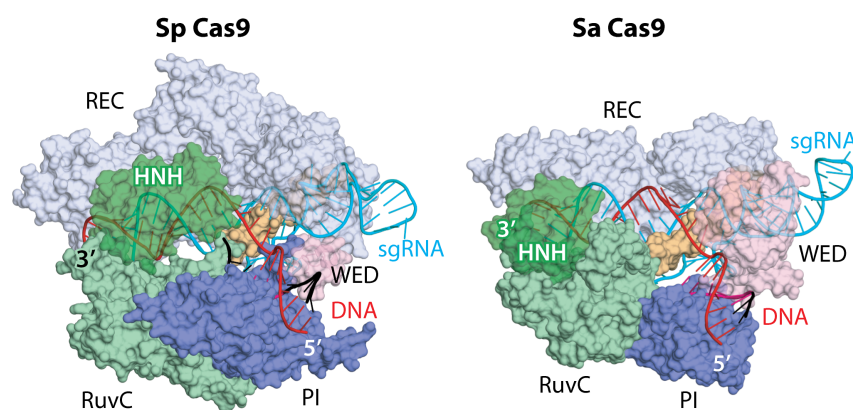


Figure 1.2. Structural models of *S. pyogenes* and *S. aureus* Cas9 in their holo forms.
(Adapted from Wang *et al.*, 2016)

1.6. Applications of the CRISPR/Cas9 System

The basic system of Cas9 and sgRNA has been used for a broad array of eukaryotic genome editing applications within medical, biotechnological and agricultural settings (Hsu

et al., 2014). SpCas9 is the most commonly used variant, and the desired genomic loci can be targeted by designing complementary sgRNA molecules. After the enzyme cleaves the targeted loci, the cell can attempt to repair the DSB through NHEJ or HDR. Alternatively, a donor DNA fragment can be provided to serve as a template to fill the gap, offering the possibility of swapping the endogenous gene with an exogenous fragment to correct deleterious mutations (Ormond *et al.*, 2017).

With the enhanced understanding of Cas9 structure and function came the possibility of artificially modifying the CRISPR system to develop novel applications, all of which take advantage of the enzyme's ability to bind to a particular genomic region under the guidance of a given sgRNA (Doudna and Charpentier, 2014). One such application, called CRISPR interference (CRISPRi), relies on an enzymatically-inactivated Cas9 variant that is referred to as dCas9 (Qi *et al.*, 2013). dCas9 contains point mutations in its RuvC1 and HNH domains, and therefore cannot execute the catalytic cleavage of dsDNA (Qi *et al.*, 2013). The binding of the dCas9-sgRNA can disrupt transcriptional elongation at a target gene. It can also hinder RNA polymerase and transcriptional activator access, essentially causing gene silencing without destroying the target (Qi *et al.*, 2013).

A major approach in the development of Cas9-based biotechnological applications centers around creation of multidomain proteins in order to combine the activities of multiple enzymes. Multidomain proteins can be crafted by either creating an end-to-end linkage by connecting the N- and C- terminals of two separate proteins via a peptide link or performing domain insertion by splicing one domain into another (Ostermeier, 2005). This approach has been used to reduce nonspecific, off-target binding of Cas9 by linking two dCas9 proteins to FokI nuclease domains, whose endonucleolytic activity requires dimerization (Tsai *et al.*, 2014). When the dCas9 proteins recognize their sgRNA-programmed loci, which are in sufficient proximity by design, the individual FokI domains dimerize and induce a DSB at the region halfway between the two dCas9 proteins. As this system depends on the simultaneous recognition of two distinct genomic regions, targeting specificity is exponentially improved (Tsai *et al.*, 2014). Furthermore, scientists have generated end-to-end fusion chimeras of dCas9 and several deaminases for precise base editing applications without necessitating any cleavage events, also putting CRISPR/Cas9 into use as a precise cargo delivery system (Komor *et al.*, 2016; Gaudelli *et al.*, 2017).

Researchers are also able to reversibly modulate the regulation rather than sequence identity of endogenous target genes by altering the epigenomic landscape. Such epigenome editing has been achieved by creating a dCas9:sgRNA construct linked to a transcriptional activator, such as VP64, which is capable increasing target gene transcription and independently inducing a relaxed chromatin conformation (Maeder *et al.*, 2013; Polstein *et al.*, 2015). Similarly, a Cas9-DNA methyltransferase (DNMT3A) fusion product can promote CpG methylation within the immediate vicinity of its target region, leading to transcriptional repression (McDonald *et al.*, 2016).

Aside from its biotechnological applications, the CRISPR/Cas9 system has seen increasingly widespread implementation in clinical contexts, with multiple ongoing trials exploring its therapeutic safety and viability for several conditions including sickle cell disease (NCT03167450), advanced esophageal cancer (NCT03081715), relapsed or refractory leukemia and lymphoma (NCT03398967, NCT03166878), non-small cell lung cancer (NCT02793856), Epstein-Barr virus-associated malignancies (NCT03044743), and HIV-related hematological malignancies (NCT03164135). In addition, CRISPR proved to be a reliable, low-cost method for creation mouse models to study the pathogenic implications of specific gene ablations (Baliou *et al.*, 2018). The system has also been used to create gene knockouts and sequence deletions in induced pluripotent stem cells (iPSCs) and other primary cell lines for cell-based assays, leading to development of cancer therapies based on newly-discovered intracellular interactions (Kawamura *et al.*, 2015; Engel *et al.*, 2016; Kavlashvili *et al.*, 2016; Raza *et al.*, 2016; Singh *et al.*, 2016; Zhang *et al.*, 2016).

The concurrent application of patient-derived iPSC and CRISPR technologies constitutes a particularly potent therapeutic weapon which scientists can wield with great flexibility to generate transplantable stem cell populations carrying desired genetic alterations. For instance, by using the CRISPR/Cas9 system on iPSCs, researchers have successfully reverted chromosomal inversions involving the *F8* gene, whose disruption leads to hemophilia A (Park *et al.*, 2015). When engrafted into mice, the “corrected” iPSCs differentiated into endothelial cells and rescued the disease phenotype. The ability of iPSCs to differentiate into all three cell layers (endoderm, mesoderm and ectoderm) immensely expands therapeutic possibilities, while their autologous transplantation eliminates the immune incompatibility concern (Singh *et al.*, 2015). A similar approach combining the

CRISPR and iPSC technologies has been adopted to correct pathogenic mutations in various other contexts including β -thalassemia (Xie *et al.*, 2014) and cystic fibrosis (Firth *et al.*, 2015).

The CRISPR system can also be used to edit human germline or embryonic cells, and as the resultant genetic modifications can be passed on to future generations, the ethical implications of such interventions are hotly debated (Mo, 2015). The first reported attempt to perform gene editing was by Junjiu Huang of Sun Yat-Sen University and resulted in an excess number of off-target mutations in nonviable zygotes, hinting at the dangers of premature applications in humans (Liang *et al.*, 2015). Two years later, arguably the most successful application of CRISPR-Cas9-mediated genome editing in human embryos was announced, with researchers correcting a heterozygous *MYBPC3* mutation that is implicated in hypertrophic cardiomyopathy (Ma *et al.*, 2017). The repaired embryos demonstrated low mosaicism and a preferential use of HDR in response to DSBs, along with a low incidence of off-target mutations. In 2018, another group in China performed dCas9-deaminase-mediated base editing in human embryos and corrected a point mutation causing Marfan syndrome with high efficiency and no observed off-target effects or indel formation (Zeng *et al.*, 2018).

1.7. Practical and Potential Issues of the CRISPR/Cas9 System

Since the initial applications for genome editing in 2013, the use of CRISPR/Cas9 has spread like a wildfire, at times appearing to outpace the contemporaneous knowledge regarding its risks and implications. The most striking demonstration of just how far some scientists are willing to go was given by He Jiankui of the Southern University of Science and Technology in China, who recently shocked the scientific community by announcing the birth of the world's first CRISPR-edited babies (Cyranski and Ledford, 2018). Despite this haste in widening the system's applications, there are numerous issues that need to be contended with, including deleterious off-target mutations and mosaicism.

Off-target cleavage events can occur as a result of nonspecific sgRNA recognition of non-targeted genomic regions due their sequence similarity to the target region (Hsu *et*

al., 2013). Similarly, the 3-nucleotide-long PAM sequence is also abundant in genomic regions, conferring a small degree of promiscuousness to Cas9 binding (O'Geen *et al.*, 2015). Multiple successful strategies have been developed to reduce the CRISPR/Cas9 off-target effects, such as creating single amino acid mutant variants that carry less positive charge in their DNA-interacting domains, with the aim of eliminating nonspecific electrostatic attractions between the enzyme and the negatively-charged DNA backbone (Slaymaker *et al.*, 2016). Another approach involves temporal restriction of Cas9 activity, so that the ribonucleoprotein complex does not linger around for long after on-target locus modification (Davis *et al.*, 2015; Zetsche *et al.*, 2015). Stipulating two independent Cas9 binding events for target cleavage to occur, as in the case of the dCas9-FokI fusion system introduced above, can also reduce off-target events (Tsai *et al.*, 2014). However, while these diverse strategies may lower off-target events to acceptable levels for many research applications, their successful execution did not entirely abate the concerns of genotoxicity when it comes to human genome-editing. A recent publication used long-range genotyping to show that CRISPR/Cas9 may cause more extensive and potentially deleterious genomic rearrangements than earlier thought, including inversions and large deletions that could have been missed with previously used short-range analyses (Kosicki *et al.*, 2018). Other findings suggest that Cas9-mediated genome editing results in DNA damage that engenders a p53-dependent response and growth arrest (Haapaniemi *et al.*, 2018). Therefore, future therapeutic applications will benefit from a more nuanced understanding of CRISPR/Cas9-induced DNA damage and the subsequently activated intracellular response pathways.

The use of CRISPR-Cas9 in the cleaving embryos may also engender mosaicism, where a subpopulation of cells possesses a distinct genomic makeup compared to the rest of the embryo (Yen *et al.*, 2014; Mehravar *et al.*, 2018). Mosaicism in this case may arise due to several factors, including an inefficiency or absence of editing in some of the constituent cells, or an overabundance or persistence in expression of the CRISPR-Cas9 ribonucleoprotein which may cause stochastic off-target genomic damage in different cells and lead to genomic divergence (Mehravar *et al.*, 2018; Tu *et al.*, 2017). Scientists have developed multiple strategies to counter this problem, such as optimization of the timing, delivery method and concentration of the CRISPR-Cas9 components (Mehravar *et al.*, 2018). For instance, co-injection of the ribonucleoprotein along with sperm into human oocytes during fertilization was observed to result in only a single case of mosaicism in the 42 embryos that were included in the study (Ma *et al.*, 2017). While these results are

encouraging, mosaicism remains to be a significant challenge for germline or embryonic editing applications. The present genotyping methods used to evaluate of the mosaicism status are predicated on the destruction of the embryo, and they are not sensitive enough to detect the smaller mutations in the genome, possibly underestimating the rates of mosaicism (Mehravar *et al.*, 2018). Furthermore, none of the current genome editing methods has consistently demonstrated an absence of mosaicism in the treated embryos, jeopardizing human applications (Mehravar *et al.*, 2018).

Another issue that limits human applications is the relative lack of control in regard to which intrinsic molecular repair pathway gets activated in the cell in response to the CRISPR-mediated endonucleolytic activity. As explained above, a DSB can be resolved through HDR and NHEJ, the latter of which is more efficient yet prone to creating random indel mutations at the damaged site (Rouet *et al.*, 1994; Choulika *et al.*, 1995; Jeggo, 1998). For this reason, and due to the ability of the HDR to incorporate an exogenous “donor” template sequence into the breakage site, many researchers have attempted to develop strategies to prod the cells towards this pathway as part of genome-editing applications (Ormond *et al.*, 2017). The preference for HDR vs. NHEJ can change depending on the cell cycle stage, and HDR efficiency can be increased if DNA damage machinery is activated during S and G2 phases (Heyer *et al.*, 2010; Yang *et al.*, 2016). Consequently, scientists have had success with fusing Cas9 to Geminin, a substrate of the cell-cycle-modulating APC/Cdh1 ubiquitin ligase complex (Gutschner *et al.*, 2016; Howden *et al.*, 2016). As a result, the fusion product gets ubiquitylated and degraded during the G1 phase when the ligase complex is maximally active, and Cas9 endonucleolytic activity remains restricted to S, G2 and M phases, dramatically increasing the HDR efficiency (Gutschner *et al.*, 2016). Another approach exploits the chemical modulators of the DSB repair pathways to selectively promote CRISPR-mediated HDR (Maruyama *et al.*, 2015; Yu *et al.*, 2015; Li *et al.*, 2017). The effectiveness of these interventions within a human embryonic or germline editing context has yet to be explored; however, it has also been suggested that human zygotes may inherently favor HDR over NHEJ, unlike iPSCs and somatic cells (Ma *et al.*, 2017).

A recent preprint article also highlighted the potential dangers of delivering a bacterial protein into humans for treatment purposes, harking back to the immunogenicity

problem that plagued gene therapy in its early days (Charlesworth *et al.*, 2018). Although the article has not gone through peer-review process as of the publication of this thesis, it reports pre-existing immunity against Cas9 in 34 human donors, with antibodies being detected against *Staphylococcus aureus* Cas9 (SaCas9) and SpCas9 in 65% and 79% of the tested blood samples, respectively. While these findings may be expected due to the ubiquitous presence of these bacteria in human tissues, Charlesworth *et al.* also report the presence of interferon- γ -secreting anti-SaCas9 cytotoxic T-cells in nearly half of the donor samples, raising the possibility that the immune system may attack the CRISPR-edited cells that express this Cas9 homologue, which may negate the therapeutic intervention or potentially trigger a systemic immune response (Charlesworth *et al.*, 2018). Therefore, proper risk assessment and prevention strategies need to be in place to maximize long-term safety and efficacy of therapies based on CRISPR-Cas9-mediated gene editing.

1.8. Posttranslational Regulation of Cas9

The previous section touched upon many hurdles facing the clinical applications of CRISPR/Cas9. I also discussed the increasingly-sophisticated interventions established to counter them. However, despite the growing body of scientific literature that examines how the Cas9 enzyme's activity might influence cellular processes, we lack the fundamental knowledge regarding how these processes might in turn influence Cas9. Future development of safe and effective therapeutic approaches is predicated on the completion of this missing piece of the puzzle, and for this reason, this project focuses on uncovering the posttranslational regulatory mechanisms of Cas9.

Proteins undergo a wide extent of reversible covalent modifications in the cell, which can dynamically change their localization, function, interaction partners, or stability (Duan and Walther, 2015). These post-translational modifications (PTMs) are thought to play a more prominent role in eukaryotes compared to prokaryotic organisms, both in terms of modification diversity and frequency (Walsh *et al.*, 2005). Eukaryotic PTMs include phosphorylation, ubiquitylation, acetylation, sumoylation, methylation and glycosylation among others (Prabakaran *et al.*, 2012). While proteins in bacteria can also undergo many of these PTMs, such as phosphorylation, acetylation, glycosylation and methylation, other types of PTMs such as sumoylation are entirely absent in the prokaryotic repertoire

(Ravikumar *et al.*, 2015; Wimmer *et al.*, 2012). Curiously, the small peptide ubiquitin has a functional bacterial analog in the prokaryotic ubiquitin-like protein (Pup), which also tags target proteins for degradation (Cain *et al.*, 2014).

To date, no covalently-linked PTMs have been reported on the Cas9 protein, either in a prokaryotic or eukaryotic setting. Our group has previously identified multiple candidate *in silico* SUMO attachment sites and confirmed that Cas9 undergoes sumoylation using multiple cell lines, which constitutes the first PTM ever identified on this protein to our knowledge. Furthermore, I was able to show that Cas9 gets ubiquitylated, and my preliminary data suggest that Cas9 ubiquitylation entails a proteasome-dependent degradation. In the next two sections, I will briefly discuss these two PTMs and their implications for target proteins.

1.9. Ubiquitylation

As its name suggests, ubiquitylation is a ubiquitous PTM in the eukaryotic cell, with its substrates being involved in almost all eukaryotic cellular processes (Swatek and Komander, 2016). The eponymous ubiquitin is a small peptide comprised of 76 amino acids and forms reversible isopeptide bonds with suitable target lysine (Lys) residues (Swatek and Komander, 2016). This bond formation is a three-step process, where each step is catalyzed by a distinct enzyme (Swatek and Komander, 2016) (Figure 1.3). The first step involves the catalytic cleavage of the carboxyl (C) terminus of the ubiquitin protein, which exposes a terminal diglycine (GG) residue and enables thioester linkage formation to the E1 ubiquitin-activating enzyme in an ATP-dependent manner (Haas *et al.*, 1982; Michael Rape, 2017). Next, the activated ubiquitin peptide gets transferred to an E2 ubiquitin-conjugating enzyme (Michael Rape, 2017). In the final step, an E3 ligase coordinates the attachment of the ubiquitin to a target protein (Michael Rape, 2017). While the ubiquitylation machinery contains multiple enzymes that are able to participate in each step, the E3 ligases constitute the most diverse group, with more than 600 predicted members (Michael Rape, 2017). Since they recruit the substrate proteins, target specificity is determined by the identity of the E3 enzyme involved (Michael Rape, 2017). Another class of enzymes called deubiquitinases (DUBs) includes specialized proteases dedicated to reversing this modification (Komander *et al.*, 2009).

Interestingly, the ubiquitin peptide itself contains seven Lys residues that are subject to ubiquitin attachment, and multiple ubiquitin proteins can be also connected to each other via their amino (N) termini (Michael Rape, 2017). This enables the formation of ubiquitin chains possessing different topologies that portend distinct fates for the target proteins (Figure 1.3). For instance, a target protein can be linked to a single ubiquitin (monoubiquitylation), which usually changes the binding partner profile (Michael Rape, 2017). Alternatively, ubiquitin peptides can form polymeric branches on the target protein via their 11th or 48th Lys residues (K11 or K48), leading to its proteasome-mediated degradation (Chau *et al.*, 1989; Mark Hochstrasser, 1996; Meyer and Rape, 2014). Another frequent ubiquitin chain formation (polyubiquitylation) pattern is established via K63 polymerization and performs nondegradative roles, such as modulating DNA repair and regulating protein kinase activity in key cellular signaling pathways such as IL-1, NF- κ B (Chen and Sun, 2009). Moreover, ubiquitin can also be modified via other PTMs such as sumoylation, acetylation and phosphorylation, further expanding the complexity of its modification patterns and functional repertoire (Swatek and Komander, 2016).

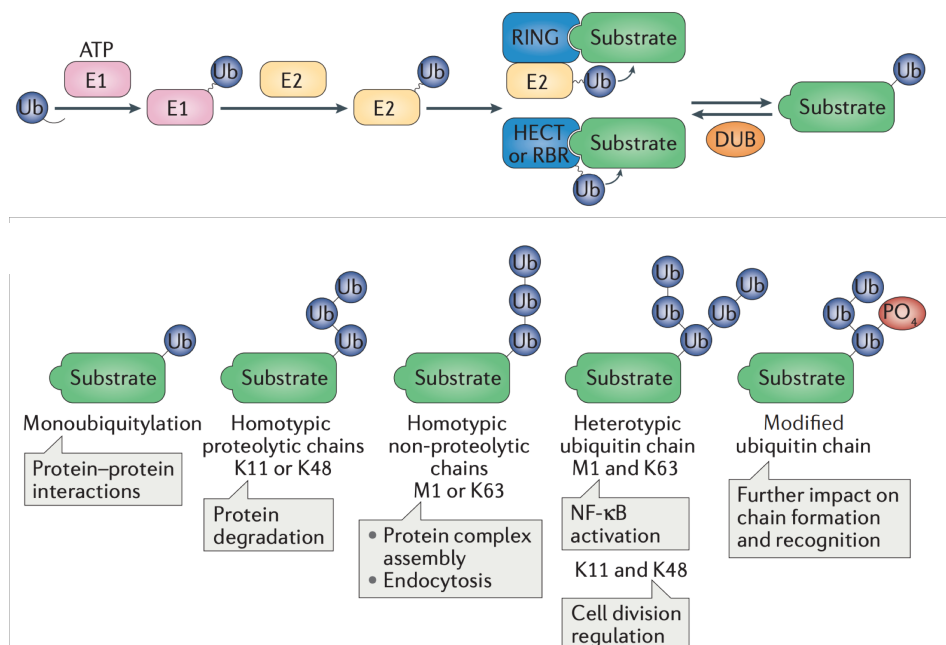


Figure 1.3. Enzymatic machinery and functional outcomes of ubiquitylation (Adopted from Michael Rape, 2017)

1.10. Sumoylation

Another ubiquitin-like eukaryotic peptide that is capable of substrate modification is SUMO (small ubiquitin-related modifier). All eukaryotes express at least one SUMO isoform, and multiple paralogues are found in vertebrates. SUMO1, SUMO2, and SUMO3 are known to play diverse roles within the cell, and the latter two are generally grouped together as SUMO2/3 due to their extremely high sequence identity (98%) and seemingly identical functions (Wimmer *et al.*, 2012). In contrast, SUMO1 has around 48% sequence similarity to SUMO2/3, although the three proteins have common features, such as a partial (~18%) sequence homology to ubiquitin, as well a shared target motif and enzymatic machinery (Jürgen Dohmen, 2004; Wimmer *et al.*, 2012; Hendriks and Vertegaal, 2016) (Figure 1.4).

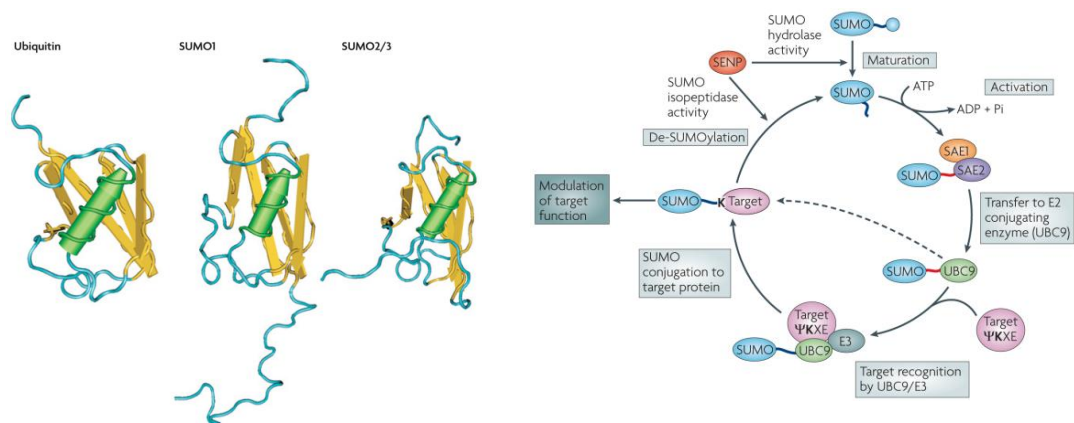


Figure 1.4. Structural comparison of modifier peptides and the SUMO machinery.

(Adopted from Martin *et al.*, 2007)

Similar to ubiquitylation, SUMO proteins are attached to target Lys residues in a three-step ATP-dependent process, with the participation of a different set of E1, E2 and E3 enzymes that were initially characterized in *Saccharomyces cerevisiae* (Jürgen Dohmen, 2004). SUMO proteins undergo maturation to become compatible for target attachment by SUMO-specific proteases which cleave the C terminus of the peptide to expose a diglycine

residue (Ronald Hay, 2005). The mature protein undergoes adenylation by a heterodimeric E1 complex consisting of SAE1 and SAE2 in humans (Ronald Hay, 2005). In the second step, the activated SUMO gets transferred to the SUMO conjugating E2 enzyme, called Ubc9, via a trans-esterification reaction (Ronald Hay, 2005). Remarkably, the Ubc9 protein is the only E2 enzyme within the sumoylation machinery and can select the specific SUMO substrate without the help of an E3 enzyme (Ronald Hay, 2005). Therefore, following the conjugation of SUMO, Ubc9 can directly catalyze its attachment to the ϵ -amino group of the target Lys via an isopeptide linkage (Ronald Hay, 2005). This Lys residue is generally included in a canonical recognition motif consisting of ψ KxE, where ψ signifies a large hydrophobic residue, and x stands for any amino acid (Ronald Hay, 2005). Nevertheless, barring a few known exceptions such as the sumoylation of RanGAP1, a specific E3 ligase is usually involved in the transfer of SUMO protein to its target and serves to increase the catalytic efficiency of this reaction (Flotho and Melchior, 2013). As with ubiquitin, SUMO can be deconjugated through the action of proteases, making sumoylation a reversible PTM (Hickey *et al.*, 2012). Also similarly, SUMO2/3 possesses an acceptor Lys, enabling poly-SUMO chain formation (Geiss-Friedlander and Melchior, 2007).

Studies on biological systems where sumoylation is abolished through the knockout or knockdown of Ubc9 revealed the critical roles played by this process. Mice with Ubc9-knockout genotype do not survive beyond the embryonic stage and their cells display disrupted nuclear organization as well as abnormalities in chromosomal organization (Nacerddine *et al.*, 2005). This mutant phenotype hints at the essential involvement of sumoylation in central cellular pathways regulating cell cycle and genome integrity, and indeed, many key components of these pathways have been identified to undergo SUMO modification, such as DNA topoisomerase II, anaphase-promoting complex/cyclosome, and PCNA (Ronald Hay, 2005). In addition, the activities of many important transcription factors can be regulated through sumoylation, among which are the tumor suppressor protein p53, NFAT-1, and androgen receptor (Ronald Hay, 2005). While the majority of SUMO substrates are located in the nucleus, cytosolic and membrane proteins also get sumoylated, including G-protein signaling components, glucose transporters, and ion channels (Martin *et al.*, 2007).

SUMO binding can have distinct biochemical consequences for its target proteins. In the case of PML protein, SUMO2/3 chain formation was discovered to lead to its degradation through RNF4-mediated ubiquitylation (Weisshaar *et al.*, 2008), whereas SUMO1 modification influences its localization to PML nuclear bodies (Müller *et al.*, 1998). In other instances, such as in the NF- κ B inhibitor I κ B α , sumoylation may antagonize ubiquitin-dependent proteasome-mediated degradation (Desterro *et al.*, 1998). In addition, sumoylation may interfere with protein interactions, or create novel binding partners (Geiss-Friedlander and Melchior).

3. AIM OF STUDY

In this study, our overall aim is to uncover the post-translational regulatory mechanisms of the Cas9 protein within a eukaryotic setting in order to explore their practical implications for the therapeutic and biotechnological applications of the CRISPR/Cas9 system. We also aim to place these modifications in a more physiologically-relevant context, with the belief that exploring the presence of eukaryotic modifications on this prokaryotic protein may contribute to our understanding of host-pathogen interactions.

Our first specific aim is to show that Cas9 gets ubiquitylated using cell-based assays such as immunoprecipitation and histidine pulldown in HEK293 cells. By doing so, we also aim to discover the functional consequences of Cas9 ubiquitylation.

Our second aim is to show the sumoylation of Cas9 by performing live infections of THP1 cells by *Streptococcus pyogenes* and detecting the direct interactions between bacterial Cas9 and eukaryotic SUMO1 or SUMO2/3 paralogues using proximity ligation assay.

4. MATERIALS

4.1. Biological Materials

For the experiments focusing on the ubiquitylation of Cas9, we used human embryonic kidney (HEK293) cells that were kindly provided to us by Dr. Nurhan Özlü from Koç University, as well as human kidney-derived HK-2 cells. The human monocytic THP-1 cell line that we used for experiments involving live infections were a generous donation by Dr. Nesrin Özören at Boğaziçi University. HeLa cells were also used for live infections. The *Streptococcus pyogenes* isolates that were used as part of these infection experiments were harvested from patients and kindly provided to us by the microbiology laboratory of the Department of Infectious Diseases at Cerrahpaşa Faculty of Medicine.

4.2. Experimental Equipments and Devices

The tables below contain lists of the equipments, devices and disposable materials used throughout this project.

Table 4.1. Equipments and Devices.

Equipment or Device	Supplier
Autoclaves	Midas 55, Prior Clave, UK ASB260T, Astell, UK
Cell culture incubator	WTC, Binder, Germany
Carbon dioxide tank (cell culture)	Genc Karbon, Turkey
Centrifuges	Ultracentrifuge J2MC, Beckman, USA VWR CT15RE, Japan Allegra X-22, Beckman USA
Cold room	Birikim Elektrik Sogutma, Turkey
Confocal microscope	Leica SP8, USA

Table 4.1. Equipments and Devices (cont.)

Electrophoresis equipments	Mini-Protean III Cell, Bio-Rad, USA
Fluorescent microscope	Axio Observer.Z1, Zeiss, Germany
Freezers and Refrigerators	4 °C: Uğur, USS 374 DTKY, Turkey -20 °C: Uğur, UFR 370 SD, Turkey -80 °C: ULT deep freezer, Thermo, UK -150 °C: Sanyo MDF-1156, UK
Heat block	Block heater analog, VWR, USA
Ice flaker	Scotsman Inc. AF20, Italy
Inverted microscope	Z1 Axio Observer, Zeiss, USA
Laminal flow cabinet	Class II B, Tezsan, Turkey
Micropipettes	Finnpipette, Thermo, USA
Microwave oven	Arçelik, Turkey
Nanodrop	ND-1000, Thermo Fisher, USA
Oven	Gallenkamp, 300, UK
pH meter	Hanna Instruments, USA
Pipettor	S1 Pipet Filler, Thermo Fisher, USA
Power supply	EC XL 300, Thermo Fisher, USA
Rotator	ISOLAB, Germany
Rotator-mixer	Grant Instruments, UK
Shaker	Analog Orbital Shaker, VWR, USA
Softwares	Quantity One, Bio-Rad, Italy ImageJ, Image Analysis Software, NIH, USA XStella 1.0, Stella, Germany FlowJo, USA, PyMOL, USA Syngene-Genetools, UK Leica LASX, USA
Sonicator	SONOPULS, Bandelin, Germany
Vortex	VWR, USA
Water purification	WA-TECH UP Water Purification Sys., Germany

Table 4.1. Equipments and Devices (cont.)

Water purification system	UTES, Turkey
Western blot documentation system	G-BOX Chemi XX6, Syngene, UK

Table 4.2. Disposable Materials.

Material	Supplier
Cell culture petri dishes (145 mm, 100 mm, 60 mm)	TPP, Switzerland
Cell culture flask (75 cm ²) with filter screw cap	TPP, Switzerland
Cell scraper	TPP, Switzerland
Centrifuge Tubes (15 mL, 50 mL)	CAPP, Denmark
Cover slips (20 mm)	Marienfeld, Germany
Cryogenic vials (2 mL)	CAPP, Denmark
Microfuge Tubes (1.5 mL, 2 mL)	CAPP, Denmark
Micropipette tips	Axygen, USA
Multiwell plates (6-well, 12-well)	TPP, Switzerland
Nitrocellulose membrane	GE Life Sciences, England
Petri dishes	Fırat Plastik, Turkey
Pipette tips (bulk)	CAPP, Denmark
Pipette tips (filtered)	BioPointe Scientific, USA
Serological pipettes (5 mL, 10 mL, 25 mL)	CAPP, Denmark
Syringe filter units (0.22 µm, 0.45 µm)	EMD Millipore, USA
Syringes (1 mL, 5 mL, 10 mL, 50 mL)	Set Medikal, Turkey
Test tubes (0.2 mL, 0.5 mL, 1.5 mL, 2 mL)	CAPP, Denmark
Whatman filter paper-extra thick	Thermo Scientific, USA

4.3. Cell and Bacterial Culture

The following table contains the media and solutions used for cell and bacterial culturing.

Table 4.3. Growth Media and Reagents.

Material	Supplier
Agar with 5% sheep blood	BD, Germany
Doxycycline hyclate	Sigma-Aldrich
Dulbecco's Modified Eagle Medium (DMEM)	Gibco, Fisher Scientific, USA
Fetal bovine serum (FBS)	Gibco, Fisher Scientific, USA
HEPES buffered saline (HBS)	Lonza, Switzerland
Gentamicin (50 mg/mL)	GeneMark, Taiwan
Luria-Bertani (LB) broth	Caisson Laboratories, USA
Penicillin/streptomycin (100X)	Lonza, Switzerland
Roswell Park Memorial Institute (RPMI) medium	Gibco, Fisher Scientific, USA
Todd Hewitt Broth (THB)	VWR, USA
Trypsin-EDTA (0.5 mM EDTA, 0.025% Trypsin)	Gibco, Fisher Scientific, USA

4.4. Plasmids

Below is a list of the plasmids used in the experiments for this project.

Table 4.4. Plasmids.

Construct	Origin	Backbone
FLAG-Cas9 (<i>S. pyogenes</i>)	Provided by Dr. N. C. Tolga Emre	pCW
His-Ubiquitin	Provided by Dr. Hugues de Thé, Collège de France	Unknown
FLAG-pCMV	Provided by Dr. Necla Birgül	pCMV

4.5. General Kits, Enzymes and Chemicals

The following tables contain lists of the kits and chemicals that were used for this project.

Table 4.5. Kits and Reagents.

Product	Supplier
Complete Mini Protease Inhibitor Cocktail	Roche, Switzerland
Duolink® In Situ Orange Starter Kit Mouse/Rabbit	Sigma-Aldrich, USA
ECL-Femto	Thermo, USA
ECL-Pico	Thermo, USA
Ni-NTA Agarose	QIAGEN, Netherlands
PageRuler Prestained Protein Ladder	Thermo, USA
Protein A/G PLUS-Agarose	Santa Cruz Biotechnology, USA
ZymoPURE™ MidiPrep Kit	Zymo Research, USA

Table 4.6. Chemicals.

Chemical	Supplier
2-mercaptoethanol	Merck, Germany
4'6-diamidino-2-phenylindole (DAPI)	Sigma-Aldrich, USA
Acetic acid	Sigma-Aldrich, USA
Acrylamide	Bio-Rad, USA
Ammonium persulfate (APS)	AppliChem, Germany
Ampicillin	Sigma-Aldrich, USA
Bovine serum albumin (BSA)	Capricorn Scientific, Germany
Bromophenol blue	Sigma-Aldrich, USA
Calcium chloride dehydrate	Sigma-Aldrich, USA
Cycloheximide	Sigma-Aldrich, USA
Dimethyl sulfoxide (DMSO)	Sigma-Aldrich, USA
Disodium hydrogen phosphate	Merck, Germany
Ethanol	Merck, Germany
Ethylenediaminetetraacetic acid (EDTA)	Wisent Bioproducts, Canada
Glycerol	MP Biomedicals, USA
Glycine	NeoFROXX, Germany
Goat serum	Gibco, Fisher Scientific, USA
Guanidine hydrochloride	Santa Cruz Biotechnology, USA
Hydrochloric acid	Sigma-Aldrich, USA
Imidazole	Sigma-Aldrich, USA
Isopropanol	Sigma-Aldrich, USA
Kanamycin	Gold Biotechnology, USA
Methanol	Merck, Germany
MG132	Calbiochem, Germany

Table 4.6. Chemicals (cont.)

N-ethylmaleimide (NEM)	Sigma-Aldrich, USA
Nonidet P-40	Sigma-Aldrich, USA
Paraformaldehyde (PFA)	Santa Cruz Biotechnology, USA
Potassium chloride	Sigma-Aldrich, USA
Phorbol 12-myristate 13-acetate (PMA)	Santa Cruz Biotechnology, USA
Sodium chloride	Merck, Germany
Sodium dodecyl sulfate (SDS)	Merck, Germany
Sodium hydroxide	Merck, Germany
Tetramethylethylenediamine (TEMED)	Sigma-Aldrich, USA
Tris-base	Sigma-Aldrich, USA
Triton X-100	VWR, USA
Tween 20	Merck, Germany

4.6. Buffers and Antibodies

The following tables contain the recipes for the solutions, gels, and buffers, as well as a list of the antibodies used throughout this project.

Table 4.7. Solutions and Buffers.

Solution/Buffer	Content
10X Phosphate buffered saline with Tween 20 (PBS-T)	80 mM NaHPO ₄ 1.5 M NaCl 20 mM KH ₂ PO ₄ 30 mM KCl 1% Tween 20 (pH 7.4)

Table 4.7. Solutions and Buffers (cont.)

10X SDS Western blot running buffer	1% (w/v) SDS 3.03% (w/v) Tris base 11.41% (w/v) glycine in ddH ₂ O
10X SDS Western blot transfer buffer	3.03% (w/v) Tris base 11.41% (w/v) glycine in ddH ₂ O
4X Laemmli buffer	200 mM TrisHCl (pH 6.8) 8% SDS 40% glycerol 4% 2-mercaptoethanol 50 mM EDTA 0.08% bromophenol blue in ddH ₂ O
5% Stacking gel (Western Blot)	0.125 mM TrisHCl (pH 6.8) 0.1% (w/v) SDS 4% (w/v) acrylamide:bisacrylamide 0.05% (w/v) APS 0.0075% (w/v) TEMED in ddH ₂ O
7% Resolving gel (Western blot)	375 mM TrisHCl (pH 8.8) 0.1% (w/v) SDS 7% (w/v) acrylamide:bisacrylamide 0.05% (w/v) APS 0.005% (w/v) TEMED in ddH ₂ O
Buffer A (His pulldown)	6 M guanidine-HCl 0.1 M Na ₂ HPO ₄ /NaH ₂ PO ₄ (1:7 mixture) 15 mM imidazole in ddH ₂ O (final pH 8.0)

Table 4.7. Solutions and Buffers (cont.)

Buffer A/TI (His pulldown)	1 volume Buffer A 3 volumes Buffer TI
Immunofluorescence blocking & antibody solution	5% (w/v) goat serum 3% BSA in PBS
Immunoprecipitation lysis buffer	2% SDS 50 mM TrisHCl (pH 8.0) 20 mM NEM Protease inhibitor cocktail in ddH ₂ O
N-ethylmaleimide (NEM) stock solution	0.5 M N-ethylmaleimide in ethanol
Radioimmunoprecipitation (RIPA) buffer	50 mM TrisHCl 250 mM NaCl 0.5% NP-40 10% glycerol in ddH ₂ O (pH 7.2)
TI buffer (His pulldown)	25 mM TrisHCl 25 mM imidazole in ddH ₂ O (final pH 6.8)
Western blot blocking & antibody solution	5% (w/v) skim milk in PBS-T

Table 4.8. Antibodies.

Antibody	Supplier	Source	Dilution
β -Actin (#8457L)	Cell Signalling Technologies, USA	Rabbit	1:1000
Cas9 (#844301)	BioLegend, USA	Mouse	1:100
FLAG (#F3165)	Sigma-Aldrich, USA	Mouse	1:1000
6X Histidine (#sc-57598)	Santa Cruz Biotechnology, USA	Mouse	1:1000
Mouse IgG, Alexa Fluor 546 (#A-11003)	Thermo Fisher Scientific, USA	Goat	1:800
Rabbit IgG, Alexa Fluor 488 (#A-11034)	Thermo Fisher Scientific, USA	Goat	1:800
SUMO-1 (#4930S)	Cell Signalling Technologies, USA	Rabbit	1:100
SUMO-2/3 (#4971S)	Cell Signalling Technologies, USA	Rabbit	1:100
Tubulin	Santa Cruz Biotechnology, USA	Mouse	1:1000
Ubiquitin (FK2) (#BML-PW8810-0500)	Enzo Life Sciences, USA	Mouse	1:1000

5. METHODS

5.1. Cell Culture

HeLa, HK-2 and HEK293 cells were maintained in Dulbecco's Modified Eagle Medium (DMEM) supplemented with 10% fetal bovine serum (FBS) and 1% penicillin/streptomycin. They were grown in 100 mm cell culture dishes in a humidified incubator that maintained the temperature at 37°C and CO₂ levels at 5%. The cells were passaged every 2-3 days when they reached a confluency of ~90%.

THP-1 cells were maintained in suspension in Roswell Park Memorial Institute (RPMI) medium supplemented with 10% FBS and 1% penicillin/streptomycin. They were maintained in the same incubator as HEK293 cells using 75 cm² tissue culture flasks and passaged every few days upon visual confirmation of sufficient confluency.

5.2. Generation of Stable Cell Lines

HEK293 cells were seeded into 100-mm cell culture dishes and grown to 80% confluency, after which they were transfected with a pCW-Cas9 lentiviral construct. Following day, the cell medium was aspirated and replaced with fresh medium containing 25 µM of chloroquine. A mixture containing 7.5 µg of psPAX₂ and 4 µg of p-VSV-G helper plasmids along with 10 µg of pCW-Cas9 was prepared in sterile double-distilled water. 62.5 µL of 2 M CaCl₂ was then added to bring the total volume up to 500 µL. The solution was then resuspended and spinned in a microfuge. Next, an equal volume of 1X HEPES Buffered Saline Solution (HBS) was added dropwise and the mixture was vigorously resuspended. After a 10-minute incubation at room temperature, the mixture was added onto the cells in a dropwise manner. Following a 6-hour incubation in the cell culture incubator, the cell medium was removed and replaced with DMEM supplemented with 10% FBS and 1% penicillin/streptomycin (complete medium). 72 hours after transfection, the cell medium was collected and passed through a 0.45 µm filter to harvest the lentivirus. The filtered medium was aliquoted into microfuge tubes to be used for lentiviral transduction.

150,000 HEK293 cells were seeded into 6-well cell culture dishes for lentiviral transduction. Next day, the lentivirus-containing medium was mixed with polybrene to obtain a final concentration of 4 $\mu\text{g}/\text{mL}$. The cell media in the 6-well plates was aspirated and replaced with 300 μL of lentivirus-containing medium. This medium was removed after 6-8 hours and fresh complete medium was added onto the cells. The transduced cells were then selected for by the addition of 2 $\mu\text{g}/\text{mL}$ of puromycin, until all untransduced cells were dead.

5.3. Transfection

HEK293 cells were transfected the day after being seeded into 100 mm cell culture dishes, when they reached a confluency of 50-70%. For each plate, 420 μL of ddH₂O was aliquoted into 1.5 mL microfuge tubes, to which 18 μg of plasmid DNA was added, followed by vortexing and a brief centrifugation step. Following this, 61 μL of 2 M calcium chloride (CaCl₂) solution was added dropwise, and the mixture was left to incubate at room temperature for 5 minutes. Next, 500 μL of 2X HBS was added dropwise. The resultant \sim 1 mL transfection mixture was vigorously resuspended and left to incubate at room temperature for 10 minutes. After incubation, the mixture was resuspended and distributed in a dropwise manner onto the cells. Concurrently with transfection, doxycycline was added to the medium with a final concentration of 2 $\mu\text{g}/\text{mL}$, as the Cas9 expression plasmid is doxycycline-inducible.

The cells were incubated for at least 18 hours before lysis to allow for optimal expression.

5.4. Histidine Pulldown Assay

For histidine pulldown experiments, HEK293 cells were grown in 100 mm dishes to a confluency of \sim 90% for lysis. The day before lysis, cells were transfected as described above with His-ubiquitin, FLAG-Cas9 and FLAG-pCMV constructs (Table 5.1), except for the stable cell line for which FLAG-Cas9 transfection was not performed. The FLAG-pCMV construct was used to equalize the amount of transfected DNA. A few hours after

transfection, cells were treated with 2 μ M of MG132 or an equal volume of DMSO as carrier. The treatment was continued overnight (~16 h).

Table 5.1. Transfection and Treatment Plan for Histidine Pulldown.

Plate #	Plasmid	Treatment
1	10 μ g His-ubiquitin + 8 μ g FLAG-pCMV	MG132
2	8 μ g Flag-Cas9 + 10 μ g FLAG-pCMV	MG132
3	8 μ g Flag-Cas9 + 10 μ g His-ubiquitin	MG132
4	8 μ g Flag-Cas9 + 10 μ g His-ubiquitin	DMSO

The following day, 50 μ L of Ni-NTA slurry was equilibrated for each experimental group. For equilibration, 1 mL of Buffer A was added to the Ni-NTA beads in a 1.5 mL microfuge tube. Next, the tube was spinned in a room temperature microfuge for 45 seconds. The supernatant was removed, and the wash was repeated two more times.

After the beads were equilibrated, the cell medium was aspirated, and the cells were quickly washed with 5 mL of 1X PBS. The PBS was removed, and another wash was performed with a 20 mM NEM solution in cold PBS. After this solution was removed, 1 mL of ice-cold PBS was added to each plate. The cells were scraped, transferred to 1.5 mL microfuge tubes and centrifuged for 45 seconds at maximum speed. The supernatant was removed, and the cells were resuspended in 500 μ L of PBS. 20 μ L of this suspension was set aside and lysed in 50 μ L of 2X Laemmli buffer to serve as whole cell lysate control. The lysate was boiled at 95 $^{\circ}$ C, centrifuged for 10 minutes at 4 $^{\circ}$ C at maximum speed, and stored at -20 $^{\circ}$ C until Western blotting.

The remaining cell suspension was spinned for 45 seconds at maximum speed, and after the supernatant were removed, the cells were lysed in 1 mL of Buffer A. Afterwards, the lysate was sonicated until it was no longer viscous. 50 μ L of equilibrated Ni-NTA beads were added to each lysate, and the mixture was incubated on a rotator-mixer at room

temperature for 3 h. After the incubation was over, the tubes were centrifuged for 10 seconds at maximum speed, and all but the last 100 μ L of the supernatant was discarded. The remaining resin was resuspended in 1 mL of Buffer A, and after a 10 second centrifugation at maximum speed, 1 mL of the supernatant was discarded. This wash step was repeated once more with Buffer A, after which two washes were performed with Buffer A/TI and one additional wash was performed with TI Buffer. After the wash, a 26G needle was inserted into the resin pellet to remove any residual liquid, and the dry resin was resuspended in 100 μ L of 2X Laemmli buffer containing 0.1 M imidazole. The lysate was boiled at 95 °C for 10 minutes, spun down for 45 seconds at room temperature, and stored at -20 °C until Western blotting.

5.5. Immunoprecipitation Assay

For immunoprecipitation, same transfection and treatment protocols were followed as described for the histidine pulldown assay (Table 5.1). Before lysis, a 100 μ L slurry of protein A/G agarose beads was set aside for each experimental group and equilibrated via 3 separate washes with RIPA buffer. The cell media were aspirated, and the cells were washed with 1 mL of 20 mM NEM dissolved in cold PBS. The solution was removed, and the cells were scraped using 1.5 mL of cold PBS and transferred into 1.5 mL microfuge tubes. After centrifugation for 1 minute at 3000 g at 4 °C, the supernatant was aspirated, and the cells were lysed using 150 μ L of cold lysis buffer consisting of 2% SDS, 50 mM Tris, 20 mM NEM and protease inhibitor cocktail. The lysis was performed by vigorously resuspending the mixture with a pipette. The lysates were then sonicated, and after ensuring sufficiently low viscosity, the lysis buffer was diluted 1:10 using RIPA buffer containing 10 mM NEM and protease inhibitor cocktail. 200 μ L of lysate from each group was collected and resuspended in 4X Laemmli buffer to serve as whole cell transfection control. The lysate mixture was boiled at 95 °C for 10 minutes, centrifuged at maximum speed for 10 minutes at 4 °C, and stored at -20 °C until Western blotting.

Next, 50 μ L of equilibrated beads were added to each of the remaining 1.3 mL lysate mixtures for preclearance to eliminate nonspecific protein binding to the beads. The bead-lysate mixtures were incubated on a rotator-mixer for 1 h at room temperature. After the incubation step was over, the microfuge tubes were spun down on a personal centrifuge

for 45 seconds at room temperature, and the supernatants were transferred to a fresh set of 1.5 mL microfuge tubes. 2.5 μ L of antibody was added into each tube, and the samples were left to incubate on a rotator-mixer for 2 h at 4 °C. Following this, 50 μ L of equilibrated beads were added into the tubes, and another 2 h incubation was performed under the same conditions. Next, the tubes were spun down, the supernatants were removed, and the bead pellets were washed 3 times with the RIPA buffer and once with cold PBS. Any remaining liquid was aspirated using a 26G syringe. After this step, the pellet was resuspended in 60 μ L of 2X Laemmli buffer, boiled at 95 °C for 10 minutes, spun for 45 seconds on a personal centrifuge at room temperature and stored at -20 °C until Western blotting.

5.6. Western Blotting

Lysates were thawed for 5 minutes at 95 °C and centrifuged before being loaded onto an SDS-PAGE gel. For the pulldown assays, 20-30 μ L of each sample was loaded onto two separate gels, accounting for the transfection and pulldown controls. After loading, electrophoresis was performed at 70 V and 130 V for the stacking and resolving portions of the SDS-PAGE gels, respectively. A protein ladder was used as reference to terminate the electrophoresis at the desired point. After this step, each gel was transferred onto a nitrocellulose membrane sandwiched between components consisting of a single thick Whatman filter paper and a cassette sponge. The enclosing cassette was placed into a wet system for the transfer step, which was carried out at 100 V for 3 h at 4 °C. Next, the nitrocellulose membranes that now contained the proteins were incubated in blocking solution (5% milk in PBS-T) for 1 h on a room-temperature shaker. After this step, the membranes were transferred into 50 mL centrifuge tubes and were supplied with the corresponding primary antibody dissolved in blocking solution. The tubes were incubated on a centrifuge tube rotator overnight at 4 °C. Next day, 3 5-minute washes were performed with PBS-T, and the membranes were treated with the secondary antibody dissolved in blocking solution. Following a 1 h room temperature incubation with the secondary antibody solution, the membranes were washed 3 times with PBS-T for 10 minutes each. Next, visualization was performed by applying a horseradish peroxidase solution directly onto the membranes, which led to a chemiluminescence signal that was detected by a visualization system (GBox Chemi, Syngene, UK).

5.7. Mass Spectrometry

MS/MS was performed to determine the ubiquitylated sites on Cas9. HEK293 cells were seeded into 100 mm cell culture dishes and transfected with FLAG-Cas9 and His-ubiquitin constructs. His pulldown was performed as described above, and the proteins were eluted by incubating the Ni-NTA beads with 120 μL of 1 M imidazole on a rotator-mixer for 2 h at room temperature, followed by another overnight incubation at 4 $^{\circ}\text{C}$. Next day, 5 μL of the elute was mixed with an equal volume of 4X Laemmli, boiled at 95 $^{\circ}\text{C}$ for 10 minutes and stored at -20 $^{\circ}\text{C}$ until Western blotting to analyze protein levels. Next, 100 μL from each elute was transferred into concentration tubes, on top of which 400 μL of RIPA buffer was added. The samples were centrifuged at 15,000 g for 5 min. When the volume above the filter was down to 100 μL , it was supplemented with another 400 μL of RIPA buffer, and this process was repeated for a total of three times. Finally, the remaining concentrated samples were transferred into a fresh set of 1.5 mL microfuge tubes, and the volume was completed to 500 μL with RIPA buffer. Again, 25 μL of the sample was set aside, mixed with 8 μL of 4X Laemmli, boiled at 95 $^{\circ}\text{C}$ for 10 minutes and stored at -20 $^{\circ}\text{C}$ until Western blotting to analyze protein levels.

Next, a protease inhibitor cocktail was added into each sample tube along with 3 μL of anti-FLAG antibody, and the samples were handled as described in the immunoprecipitation protocol starting with the lysate-antibody incubation step, except that the elution was performed using 65 μL of 2X Laemmli. The samples were then sent to the European Molecular Biology Laboratory (EMBL) for analysis.

5.8. Bacterial Culture and Infection

The number of bacteria in the suspension cultures of *Streptococcus pyogenes* was determined by inoculating the bacteria into 10 mL Todd Hewitt Broth (THB) in a 15 mL centrifuge tube and incubating the sealed tube overnight (16 h) at 37 $^{\circ}\text{C}$. Next day, the culture was retrieved, and serial dilutions were performed in THB. For each diluted suspension, an optical density measurement was obtained at 600 nm (OD_{600}) using a spectrophotometer. The suspensions were then plated on agar plates containing sheep blood and incubated

overnight at 37 °C. The following day, a colony count was performed on the blood agar plates, and the number of observed colonies was taken to be indicative of the number of bacteria in the corresponding suspension. This number was then correlated to the previously obtained OD₆₀₀ measurements so that a standard could be established for the infections to estimate the number of bacteria in a given culture based on its OD₆₀₀ value.

Before infection, *Streptococcus pyogenes* were inoculated into 10 mL of Todd Hewitt Broth (THB) and grown overnight as described in the previous paragraph. A non-inoculated THB tube was also incubated to control for contamination. Next day, the bacterial suspension was diluted 1:10 in THB into a separate subculture, and OD₆₀₀ measurement was obtained at this initial timepoint. The subculture was then incubated at 37 °C until the OD₆₀₀ value quadrupled, indicating that the bacterial growth curve had attained the log phase.

In parallel, THP-1 cells were seeded on 20 mm cover slips within 12-well plates the day before infection, with 500,000 cells being apportioned into each well. The cells were treated overnight (~18 h) with 20 ng/mL of PMA dissolved in complete RPMI in order to induce monocyte differentiation for optimal attachment and infectivity. Next day, the treatment medium was removed, and the adherent cells were washed with PBS. After the PBS was removed, 500 µL of incomplete RPMI (without FBS or penicillin/streptomycin) was added into the wells, and log phase *Streptococcus pyogenes* suspension was added dropwise onto the cells. The multiplicity of infection (MOI) was standardized at 20. After internalization was allowed to take place for 2 h in the cell culture incubator, the medium was removed, and the cells were treated with 400 µg/mL of gentamicin in incomplete RPMI for 45 minutes to kill of any extracellular bacteria. After this step, the cells were removed from the incubator and washed 3 times with PBS to remove any residual bacteria.

5.9. Immunofluorescence

Immunofluorescence experiments were performed with THP-1 cells infected as described above. For this purpose, the PBS-washed cells were fixed with 4% paraformaldehyde in PBS for 30 minutes at room temperature. The paraformaldehyde solution was removed after this time period, and the cells were washed for 5 minutes with a

300 mM solution of glycine in cold PBS to quench the free aldehyde groups and prevent nonspecific antibody binding. The glycine solution was removed, and 2 5-minute washes were performed with PBS. After this, the cells were permeabilized with 0.25% Triton-X in PBS for 30 minutes at room temperature. This solution was removed, and the cells underwent 3 5-minute washes with PBS at room temperature. After washing, a blocking solution (3% BSA and 5% goat. Serum in PBS) was added to the cells. Following two hours of blocking at room temperature, the cover slips were removed from the 12-well plates and placed upside down onto a parafilm-coated platform containing 20 μ L of the primary antibody solution (1:100 in blocking solution). The setup was transferred into a portable humidifying chamber, which was left overnight at 4 °C. Next day, the cover slips were flipped, and the antibody solution was removed via a pipette. 3 5-minute PBS incubations were performed at room temperature, after which the cover slips were placed onto the parafilm platform to be incubated with the secondary antibody solution (1:800 in blocking solution). After a 4 h incubation in a dark humidifying chamber at room temperature, the cover slips were flipped again, and the antibody solution was washed off with 3 5-minute PBS incubations at room temperature. The cover slips were then mounted onto slides using 8 μ L of Vectashield mounting medium containing DAPI, and a transparent nail polish was applied along the periphery of the cover slips. The slides were then stored at 4 °C until visualization under the confocal microscope (Leica TCS SP8, USA).

5.10. Proximity Ligation Assay

THP-1 cells were used for *in situ* proximity ligation assay following infection with *Streptococcus pyogenes* as described above. The immunofluorescence protocol was followed until after the overnight primary antibody incubation step was completed. After the cover slips were flipped, the surface containing the adherent cells was incubated 3 times in PBS-T for 5 minutes each at room temperature. In parallel, oligonucleotide-conjugated secondary antibodies were included in a solution containing 4 μ L of mouse secondary (PLUS), 4 μ L of rabbit secondary (MINUS) and 12 μ L of PLA dilution buffer for each condition. The mixture was prepared within a 0.2 mL test tube, centrifuged and vortexed. The 20 μ L mixture was then applied onto the parafilm platform, on which a cover slip was placed with the adherent cells facing down. The cells were incubated in this solution for 4 h at room temperature in a humidifying chamber. After this step, the cover slips were

incubated 5 times in PBS-T for 5 minutes each to eliminate excess antibody. During these washes, a ligation mix was prepared by diluting the 5X ligation buffer in nuclease-free sterile water to a final volume of 20 μ L per condition and adding 0.5 μ L of ligase. The mixture was gently vortexed and briefly centrifuged. When the PBS-T washes were finished, the cover slips were incubated in the ligation mixture on parafilm for 30 minutes in a humidifying chamber at 37 °C. After ligation, 5 5-minute incubations were performed in PBS-T as described in the previous step. During these washes, 5X amplification buffer was diluted in nuclease-free sterile water to yield a final volume of 20 μ L per condition, into which 0.75 μ L of polymerase was added. Once the PBS-T washes were complete, the cover slips were transferred onto the polymerization mixture on parafilm and incubated for 120 minutes at 37 °C in a humidifying chamber. Following polymerization, the cover slips were washed at room temperature with 2 10-minute incubations in 1x PLA wash buffer, followed by a final 1-minute incubation in 0.01x PLA wash buffer. The cover slips were then dried off, mounted and stored as described in the immunofluorescence protocol. All of the buffers, antibodies and enzymes used after the primary antibody incubation step were provided by the PLA kit.

The same protocol was followed for the experiments involving the endogenous ubiquitin modification in Cas9-stable HK2 cells, excluding the infection step.

6. RESULTS

6.1. Generation of the Cas9-Stable HEK293 Cells

Human embryonic kidney (HEK293) cells were transduced with a doxycycline-inducible lentiviral construct expressing FLAG-Cas9 for immunoprecipitation and histidine pulldown experiments. The Cas9 levels upon an overnight treatment with 2 $\mu\text{g}/\text{mL}$ of doxycycline were determined via Western blotting by probing with anti-FLAG antibody (Figure 6.1). Upon confirmation of sufficient protein levels, we proceeded with the experiments using this stable expression system, in parallel to experiments with a transfection-based system where the FLAG-Cas9 construct is transiently-expressed.

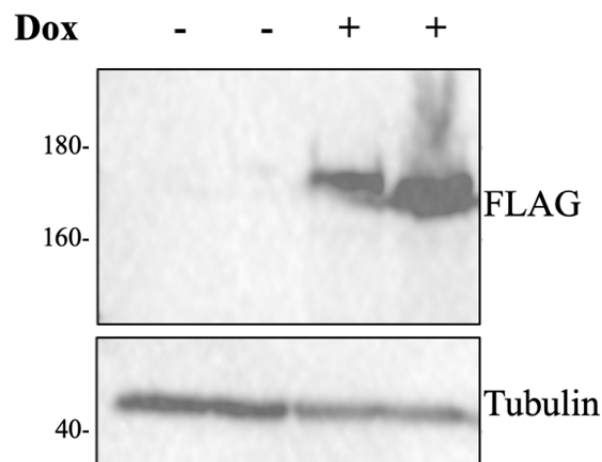


Figure 6.1. Inducible FLAG-Cas9 expression in HEK293 cells. FLAG-Cas9 expression was induced in HEK293 cells following lentiviral transduction and overnight doxycycline treatment. The cells were lysed next day, and the expression levels were determined by immunoblotting in biological duplicates. Tubulin was used as loading control. Dox = doxycycline.

6.2. Investigation of Cas9 Ubiquitylation by His Pulldown Assays

In order to investigate the potential post-translational modifications on the Cas9 protein, we started out by assaying for the covalent interactions between Cas9 and ubiquitin in HEK293 cells. Ubiquitylation often leads to decreased protein stability due to proteasomal degradation, which can be circumvented with the use of proteasomal inhibitors such as MG132 (Hayashi *et al.*, 1992). We explored whether this was the case for Cas9 by performing transfections with His-ubiquitin and FLAG-Cas9 in the presence or absence of MG132, followed by pulldown with Ni-NTA agarose beads and immunoblotting with anti-FLAG antibody. Our results revealed robust ubiquitin modification on Cas9, yielding a ladder-like pattern which suggests polyubiquitylation or ubiquitylation at multiple residues (Figure 6.2). This pattern was largely absent in the experimental group that was treated with the carrier, hinting at the degradation of modified Cas9 by the ubiquitin-proteasome system.

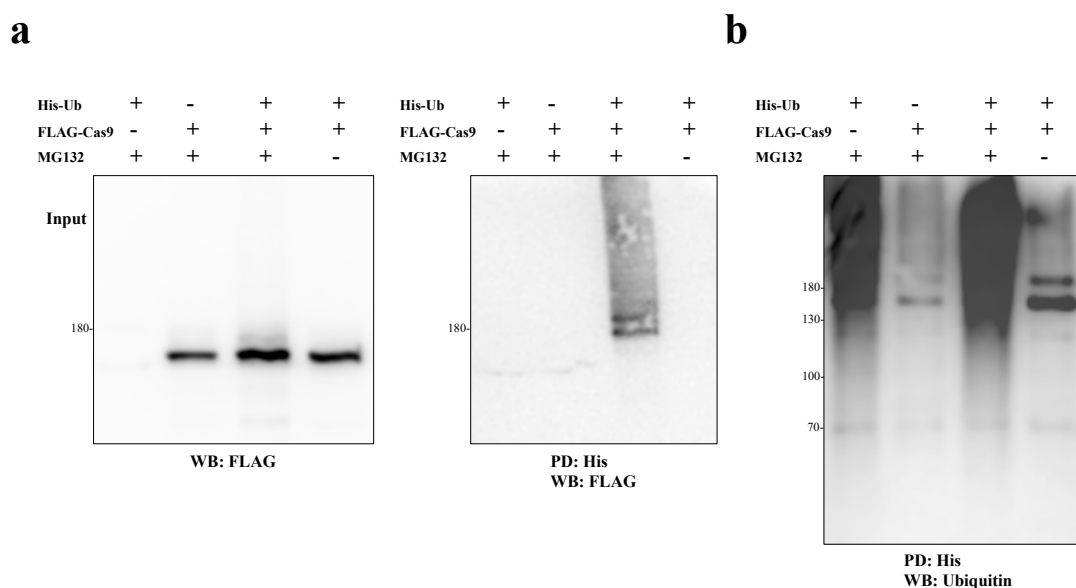


Figure 6.2. His pulldown with immunoblotting for anti-FLAG. HEK293 cells were transfected with the indicated constructs and treated with MG132 or carrier. (a) Ubiquitylated Cas9 is visible upon transfection of His-Ub and FLAG-Cas9 in combination with MG132 treatment. (b) Ubiquitin profile in the pulldown fraction. WCL = whole cell lysate. PD = pulldown.

To further verify our results, we repeated the experiment in HEK293 cells transduced with a doxycycline-inducible lentiviral vector carrying FLAG-Cas9, instead of transiently expressing this construct through transfection. As per the experimental setup that was explained above, we transfected these cells with His-ubiquitin and performed a His pulldown assay. Our results corroborated the presence of Cas9 ubiquitylation, which was not observable in the group that was treated with carrier rather than MG132 (Figure 6.3).

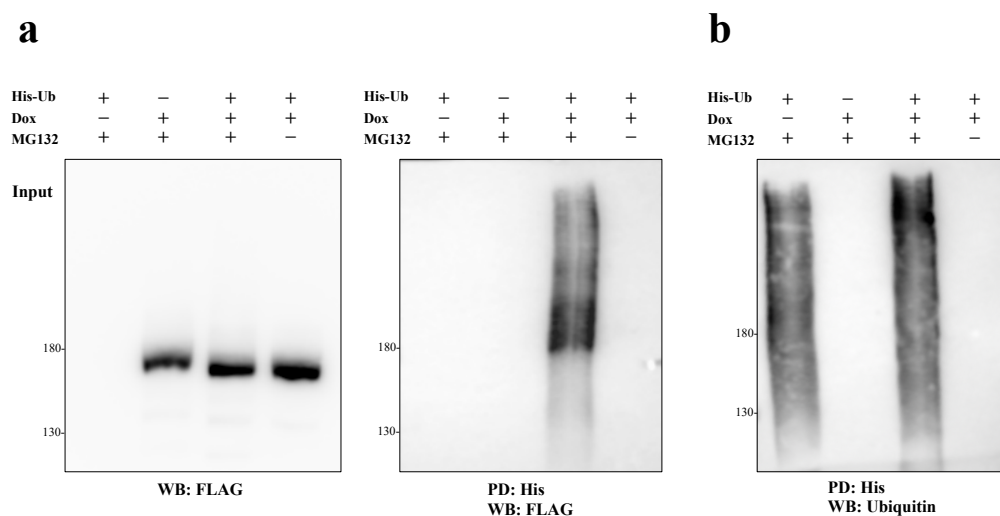


Figure 6.3. His pulldown with immunoblotting for anti-FLAG in Cas9-stable HEK293 cells. HEK293 cells were transfected and treated as indicated above. a) Ubiquitylated Cas9 is visible upon transfection of His-Ub in combination with MG132 treatment. (b) Ubiquitin profile in the pulldown fraction. Dox = doxycycline. PD = pulldown. WB = Western blot.

6.3. Investigation of Cas9 Ubiquitylation by Immunoprecipitation Assay

We tested the same idea using a different approach by immunoprecipitating FLAG-Cas9 and immunoblotting for His-ubiquitin. Once more, HEK293 cells were transfected with His-ubiquitin and FLAG-Cas9, in combination with an overnight treatment with MG132. Following pulldown with anti-FLAG antibody and immunoblotting using His

antibody, we observed a smear-like pattern in the group that was transfected with FLAG-Cas9 and His-ubiquitin under MG132 treatment condition (Figure 6.4). As before, this pattern was absent in the experimental group treated with carrier.

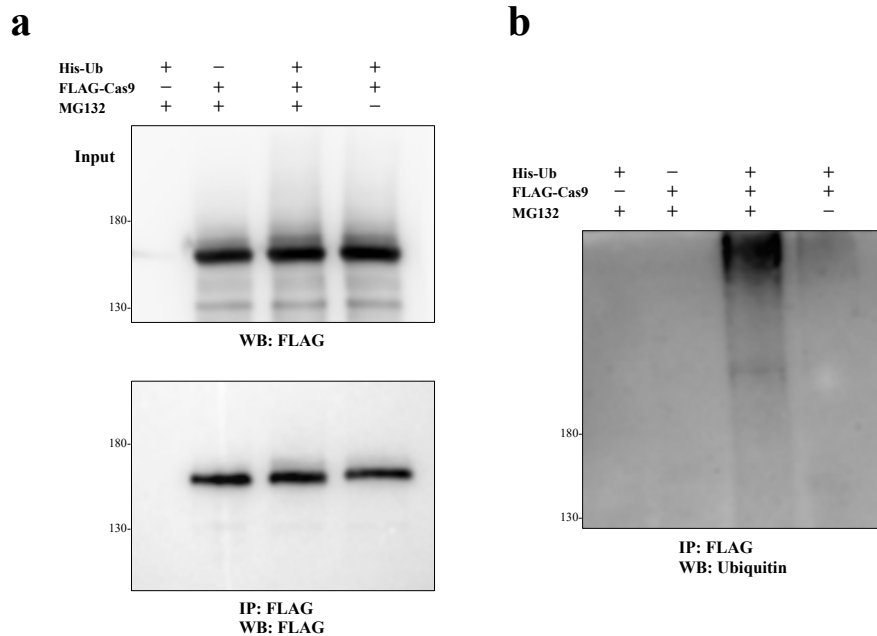


Figure 6.4. Immunoprecipitation of FLAG-Cas9 with immunoblotting for His. HEK293 cells were transfected with the indicated constructs and treated with MG132 or carrier. Next day, immunoprecipitation was performed using agarose beads coupled with anti-FLAG antibody. (a) Cas9 levels across the four experimental groups. (b) His-ubiquitin-modified Cas9. IP = immunoprecipitation. WB = Western blot.

6.4. Investigation of Cas9 Ubiquitylation by Proximity Ligation Assay

Finally, in order to further confirm our previous results in a more natural setting under stable expression conditions, we performed a proximity ligation assay (PLA) in FLAG-Cas9-stable HK2 cells to probe for the ubiquitylation of Cas9. PLA is a highly sensitive technique that enables visualization of protein-protein interactions that occur within the proximity of less than 40 nm (Sahin et al., 2016). Therefore, it affords the possibility of using endogenous levels of proteins to detect ubiquitin or SUMO

modifications, which is challenging with less sensitive methods such as immunoprecipitation.

We used antibodies that target FLAG-Cas9 and endogenous ubiquitin, and specific secondary antibodies that recognize only one of these primary antibodies. These secondary antibodies are conjugated to complementary oligonucleotides that interact when the secondary antibodies are in sufficient proximity and undergo a rolling circle amplification reaction, the product of which yields a detectable fluorescent signal. Our results corroborated the presence of ubiquitin modification on stably-expressed FLAG-Cas9 under MG132 treatment conditions in HK-2 cells (Figure 6.5). In addition, very few signals were observed in the absence of MG132, indirectly confirming the proteasomal degradation hypothesis. Negative control groups were probed with either FLAG or ubiquitin antibody, but not both, and signified the background signal level. Thus, we were able to visualize Cas9 ubiquitylation with the endogenous levels of this modifier for the first time.

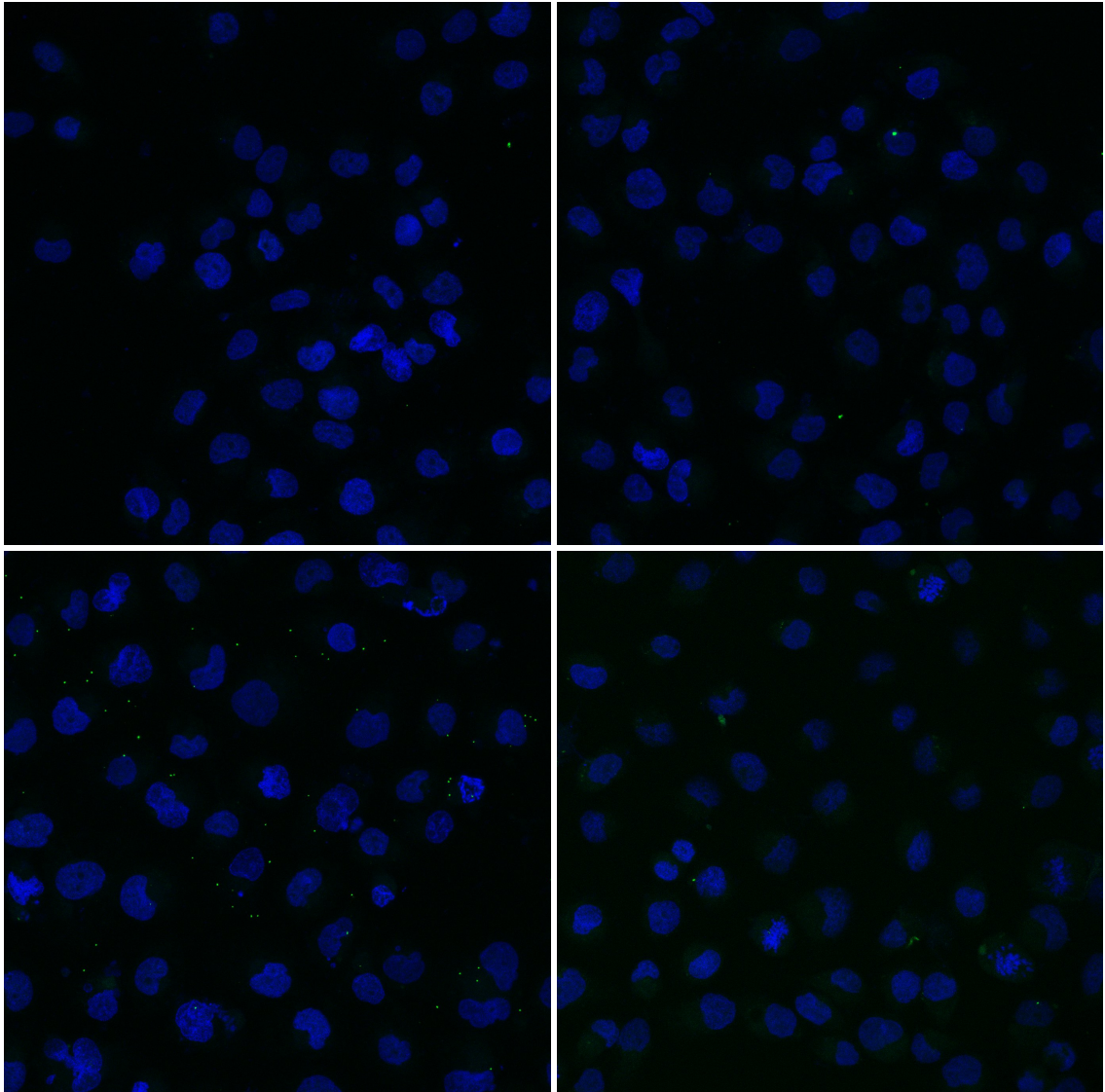


Figure 6.5. PLA in FLAG-Cas9-stable HK-2 cells showing interaction between Cas9 and endogenous ubiquitin. Clockwise starting from upper-left: FLAG-only primary antibody control (+MG132), ubiquitin-only primary antibody control (+MG132), Cas9 and ubiquitin interaction (+DMSO), Cas9 and ubiquitin interaction (+MG132).

6.5. Mass Spectrometry to Determine the Ubiquitylation Sites on Cas9

Having employed multiple approaches to assess Cas9 ubiquitylation, we moved on to mapping the ubiquitin-modified sites by performing MS/MS in FLAG-Cas9- and His-ubiquitin-transfected HEK293 cells. The samples were prepared by Yusuf Tunahan Abaci

at Bogazici University and sent to the European Molecular Biology Laboratory (EMBL) for analysis. The ubiquitin modifications on the Lys residues were detected as diglycine (GG) remnants following tryptic digestion and identified as such when the Mascot score reached a significance threshold value of ≥ 32 for the given peptide, in combination with a minimum Mascot delta score of 5 (Table 6.1). After applying these criteria, we were left with 11 sites that are subject to ubiquitylation (Figure 6.6).

Table 6.1. Ubiquitin-Modified Cas9 Residues as Determined by Mass Spectrometry.

Description	Position	Amino acid	Sequence	Score	Delta
Cas9	150	K	LEESFLVEEDKKHER	27	10
Cas9	179	K	KLVDSTDK	35	35
Cas9	186	K	LVDSTDKADLR	75	75
Cas9	271	K	LENLIAQLPGEKK	41	8
Cas9	352	K	VNTEITKAPLSASMIK	40	40
Cas9	430	K	MDGTEELLVKLNR	26	26
Cas9	538	K	MTNFDKNLPNEK	39	33
Cas9	544	K	NLPNEKVLPK	20	20
Cas9	748	K	EDIQKAQVSGQGDSL HEHIANLAGSPAIK	28	28
Cas9	893	K	DDSIDNKVLTR	28	28
Cas9	904	K	GKSDNVPSEEVVK	36	36
Cas9	934	K	KFDNLTK	24	24
Cas9	940	K	KFDNLTKAER	60	60
Cas9	986	K	YDENDKLIR	24	24
Cas9	1062	K	MIAKSEQEIGK	48	48
Cas9	1069	K	SEQEIGKATAK	41	39
Cas9	1123	K	KVLSMPQVNIVK	21	21

Table 6.2. Ubiquitin-Modified Cas9 Residues as Determined by Mass Spectrometry (cont.)

Cas9	1135	K	KTEVQTGGFSK	91	91
Cas9	1223	K	NPIDFLEAKGYK	22	10
Cas9	1260	K	MLASAGELQKGNELALPSK	56	56

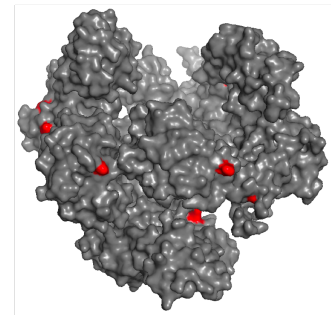
a

```

DKKYSIGLDIGTNSVGVAVITDEYKVPSSKFKVLGNTDRHSIKKNLIGALLFDSGETAEATRLKRTARRRYTRKKNR
ICYLQEIFSNEMAKVDDSFHRLSEESFLVEEDKKHERHPFGNIVDEVAYHEKYPTIYHLRKKLV DSTDKADLRLLIY
LALAHMIFRGRHFLIEGLNPDNSDVKLFIQLVQTYNQLFEENPINASGVDAKALLSARLSKSRLENLIAQLPGE
KKNGLFGNLIALSGLTPNFKSNFDLAEDAKLQLSKDYDDDLNLAQIGDQYADLFLAANKNSDAILLSDILRVN
TEITKAPLSASMIKRYDEHHQDLTLLKALVRQQLPEKYKEIFFDQSKNGYAGYIDGASQBEFFYKFKIPILEKMDGT
EELLVKLNREDLLRQRTFDNGSIPHQIHLGELHAILRRQEDFYFPLKDNREKIEKILTFRIPIYYVGPLARGNSRFA
WMTRKSEETITFPWFEEVVDKGAASQSFIERMTNFDKLNLPNEKVLPKHSLLYEYFTVYNELTKVKYVTEGMRKPAFL
SGEQKAIVDLLFKTNRKVTVKQLKEDYFKIECFDSVEISGVEDRFNASLGTYHDLKIIKDDKDFLDNEENEDILE
DIVLTLTLFEDREMIERLRTYAHLFDDKVMKQLKRRRYTGWGRLSRKLINGIRDKQSGKTLDFLKS DGFANRFM
QLIHDDSLTFKEDIQKAVSQGSDSLHEHIANLAGSPAIKKGLLQTVKVVDELVKVMGRHKPENIVEMARENQTTQ
KGGKNSRERMRKRIEEGKELGSQILKEHPVENTQLQNEKLYLYLQNGRDMYVDQELDINRLSDYDVDHIVPQSFLK
DSDIDNKVLRSDKNRGKSDNVPSEEVVKKMKNYWRQLLNAKLITQRKFDNLTKAERGGLSELDKAGFIKQVLETR
QITKHVAQILDSRMNTKYDENDKLIREVKVI TLKSKLVSDFRKDFQFYKREINNYHHAHDAYLNAVGTALIKKYP
KLESEFYGDYKVYVVRKMIAKSEQEI GKATAKYFFYSNIMNFFKTEITLANGEIRKRELITNGETGEIVWDKGRD
FATVRKVL SMPQVNI VKTEVQTGGFSKESILPKRNSDKLIARKKDWDPKKGFDSP TVAYSVLVAVKVEKGSKK
LKSVKELGITIMERSSEFKNPIDFLEAKGYKEVKKDLIKLPKYSLEFENGRKRMLASAGELQKGNELALPSKYV
NFLYLASHYEKLGKSPEDNEQKQLFVEQHKHYLDEIIIEQISEFSKRVILADANLDKVL SAYNKRHRDKPIREQAENII
HLFTLTNLGAPAAFKYFDTTIDRKRYTSTKEVLDATLIHQISITGLYETRIDLSQLGGDKRPAATKAGQAKKKK

```

b



c

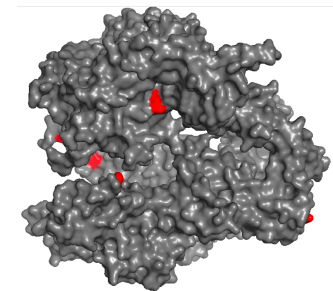
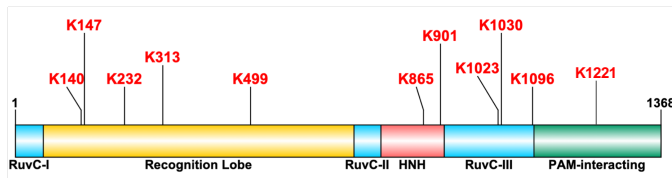


Figure 6.6. Mass Spectrometry Results Showing Ubiquitin-Modified Residues on spCas9. (a) The spCas9 amino acid sequence with the modified Lys residues highlighted in red. (b) The positions of the modified residues on the spCas9 3D model. (c) The positions of the modified residues within each domain.

6.6. Stability of the Ubiquitylated Cas9 Protein

Next, we asked how ubiquitylation-dependent proteasomal degradation impacted the half-life of Cas9. One strategy that can be used to answer this question involves mutating all ubiquitin-targeted lysines and comparing the stability of the mutated construct with that of

the wild-type one. Since we lacked the relevant mutant constructs at the time, we decided to perform a time-course analysis of Cas9 stability in the presence of absence of MG132 using Cas9-stable HK-2 cells. For this purpose, we induced FLAG-Cas9 expression in these cells through an overnight incubation with 2 $\mu\text{g}/\text{mL}$ doxycycline while simultaneously treating the cells with 2 μM MG132 or an equivalent volume of DMSO (carrier). Next day, we removed doxycycline started treatment with 50 $\mu\text{g}/\text{mL}$ of cycloheximide for all groups and collected the cell lysates at defined timepoints. The results showed that Cas9 half-life was longer than 24 hours, which was the longest timepoint we were able to pursue due to the toxic effects of cycloheximide on the cells, especially in combination with MG132 (Figure 6.7). Although the initial levels of Cas9 seem to be higher in the MG132-treated cells, later timepoints reveal lower levels of Cas9 in this group, most likely attributable to increased cell death.

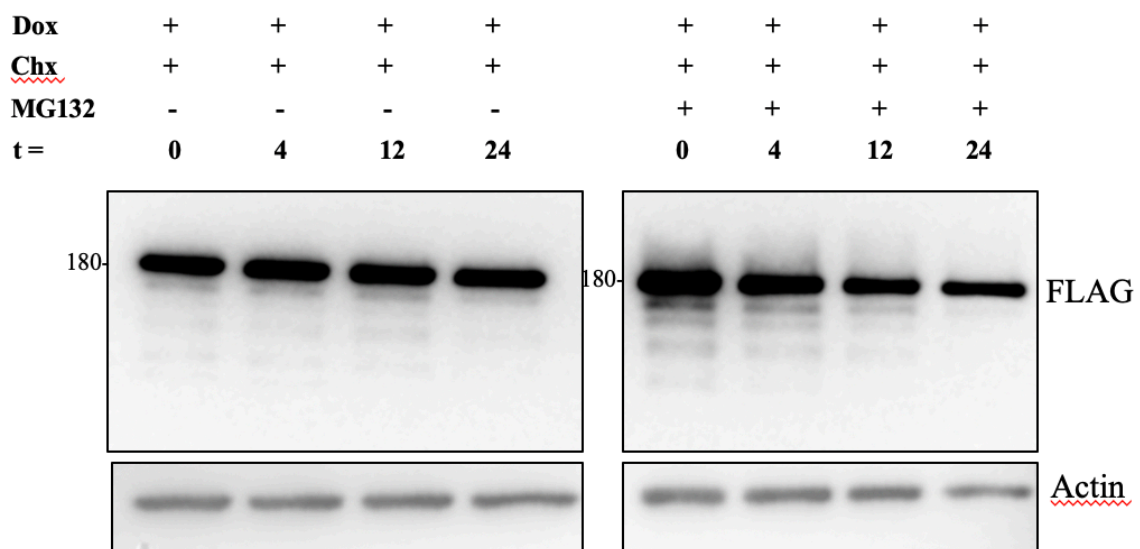


Figure 6.7. Cycloheximide chase assay to analyze Cas9 stability. Cas9-expressing HK2 cells received 50 $\mu\text{g}/\text{mL}$ of cycloheximide over the indicated time periods to assess the Cas9 half-life (left panels). The same treatment was carried out in the presence of 2 μM MG132 (right panels). Actin was used as loading control. Dox = doxycycline. Chx = cycloheximide. t = treatment duration in hours.

6.7. Infection of Human Cell lines with *S. pyogenes*

Our *in silico* analyses on the SpCas9 amino acid sequence revealed 10 candidate consensus motifs that may potentially be subject to SUMO modification (Figure 6.8). Subsequent to this finding, immunoprecipitation and proximity ligation assays by Yusuf Tunahan Abaci, another member of our group, showed that stably- and transiently-expressed Cas9 can get modified by SUMO-1 and SUMO-2/3 (unpublished data). Consequently, we wanted to explore what the implications of this eukaryotic modification on a bacterial protein were in terms of the host-pathogen interactions in nature. For this purpose, we first attempted to optimize a cell-culture-based system where we could induce infection and internalization of *S. pyogenes* by human cells, followed by an assay to test whether endogenous SpCas9 gets modified by the host SUMO machinery. This bacterium is a human pathogen that colonizes the surfaces of epithelial cells and in certain instances can invade them (Greco *et al.*, 1995). As previous literature showed that HeLa cells are particularly vulnerable to intracellular infections by *S. pyogenes* (Greco *et al.*, 1995), we first attempted to infect these cells using different multiplicities of infection (M.O.I.) between 20-200 (Figure 6.9). The cells were infected with log-phase bacteria for 2 hours and then treated with 400 µg/mL of gentamicin in RPMI for a duration 45 minutes, which we determined to be sufficient to kill all extracellular bacteria. When we lysed the infected cells with either 0.1% Triton-X in PBS, deionized water or RIPA and spread the lysate on blood agar plates, we were unable to observe any colony-forming units the following day, signifying a lack of internalization by HeLa cells. We repeated the same protocol in HK-2 cells, which also did not give rise to any colony-forming units of intracellular origin.

Given that the epithelial cell infections did not work in our hands, we decided to adopt a different approach that relied on the ability of THP-1 human monocytic cells to engulf pathogens rather than the infectivity of our *S. pyogenes* strain. For this purpose, we infected these cells using an M.O.I. of 50 for only 1 hour in order to prevent bacterial death subsequent to engulfment, followed by a 45-minute treatment with 400 µg/mL of gentamicin. Upon trying 3 different lysis protocols as described in the previous paragraph and plating the lysate that was diluted 1:5 in Todd Hewitt Broth on agar plates, we were able to observe 12 colony-forming units. Hence, we concluded that at least 60 bacteria were

internalized by THP-1 cells, which likely is an underestimation of the actual number given the bactericidal activity of these cells.

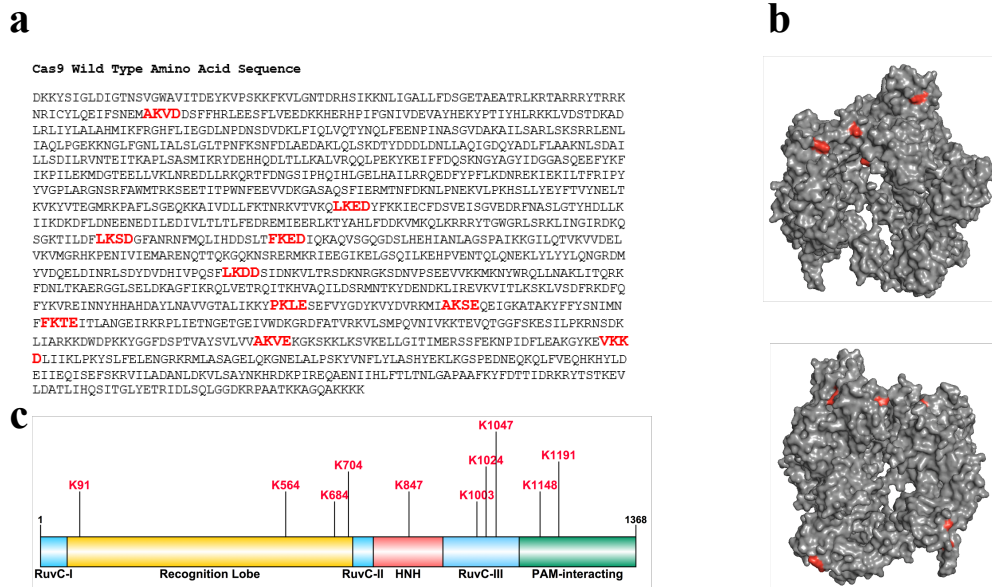


Figure 6.8. Consensus sumoylation motifs on SpCas9. (a) The SpCas9 amino acid sequence with candidate sumoylation sites highlighted in red. (b) The same sites on the SpCas9 3D model. (c) The location of each candidate site within SpCas9 domains.

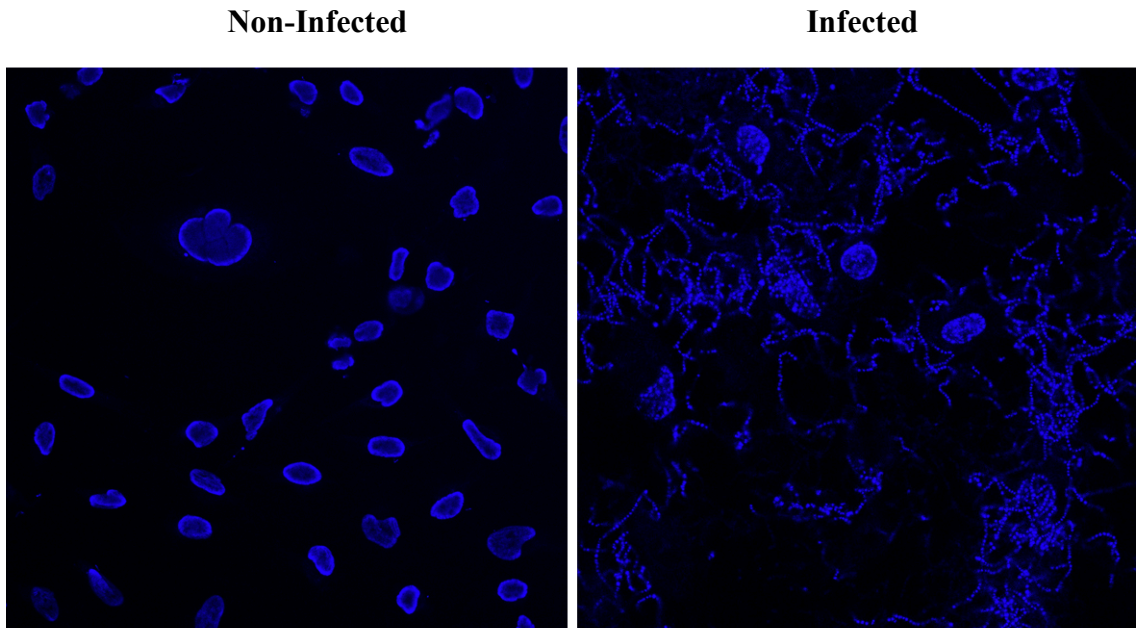


Figure 6.9. DAPI staining of HeLa cells. HeLa cells were infected with *S. pyogenes* for 2 hours, followed by a 45-minute gentamicin treatment. The filamentous and rosary bead-like Streptococcal colonies are visible in the second panel surrounding the HeLa cell nuclei.

After confirming that THP-1 cells were capable of internalizing bacteria, we proceeded with the immunofluorescence staining of SUMO proteins and Cas9, before attempting a PLA to show an interaction between these proteins. Since THP-1 are normally suspension cells that become adherent upon differentiation into macrophages, the additional incubations that we performed as part of the immunofluorescence protocol led to detachment of the cells from their culture dishes, hindering our immunolabeling efforts. For this reason, we started to treat the cells overnight with 20 ng/mL of phorbol 12-myristate 13- acetate (PMA) prior to infection, which induces THP-1 differentiation and adherence while also priming these cells for interactions with pathogens (Starr *et al.*, 2018). After the cells became sufficiently adherent, we performed infection and immunolabeling of the cells with SUMO-1 and Cas9. After optimizing the protocol to work in our system, we were able to observe SUMO-1 labeling in both non-infected and infected cells, as well as Cas9 labeling in only the infected cells (Figure 6.10). Despite these results, further experiments did not show consistent and prevalent labeling of Cas9 in these cells, although both SUMO-1 and SUMO-

2 were successfully labeled (Figure 6.11). A time-course experiment where we started the immunofluorescence protocol 4 and 5 hours post-infection also failed to yield improved Cas9 labeling (data not shown).

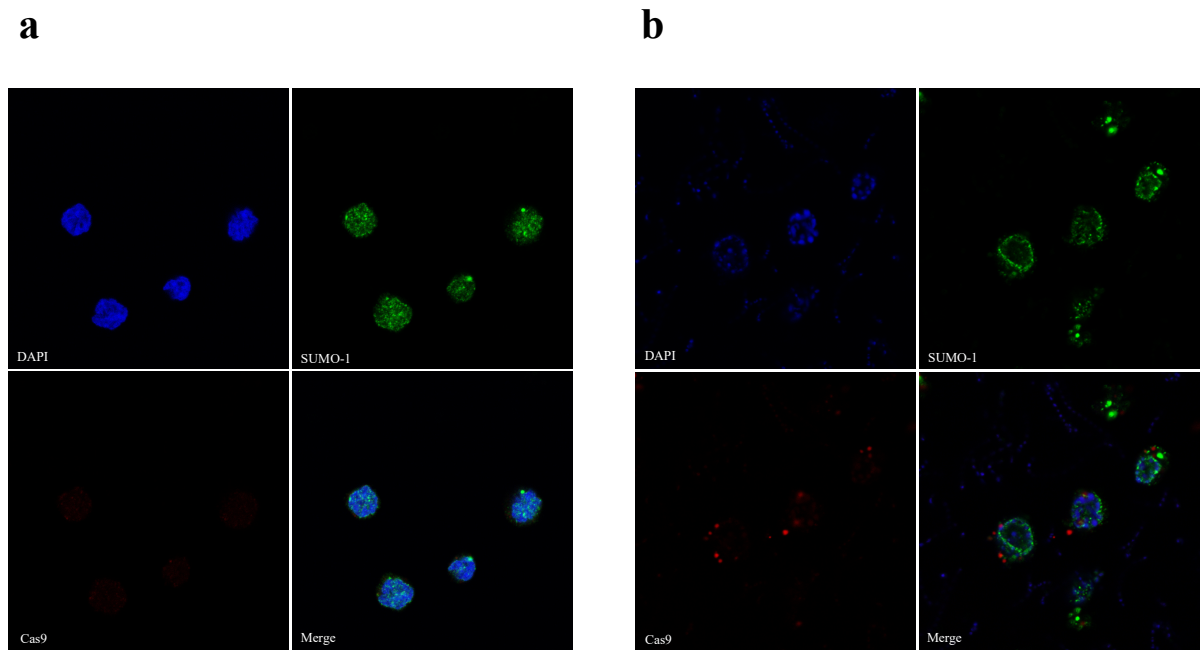


Figure 6.10. SUMO-1 and Cas9 labeling in (a) non-infected and (b) infected THP-1 cells. For each panel: upper left image = DAPI; upper right image = SUMO-1; lower left image = Cas9; lower right image = merged images.

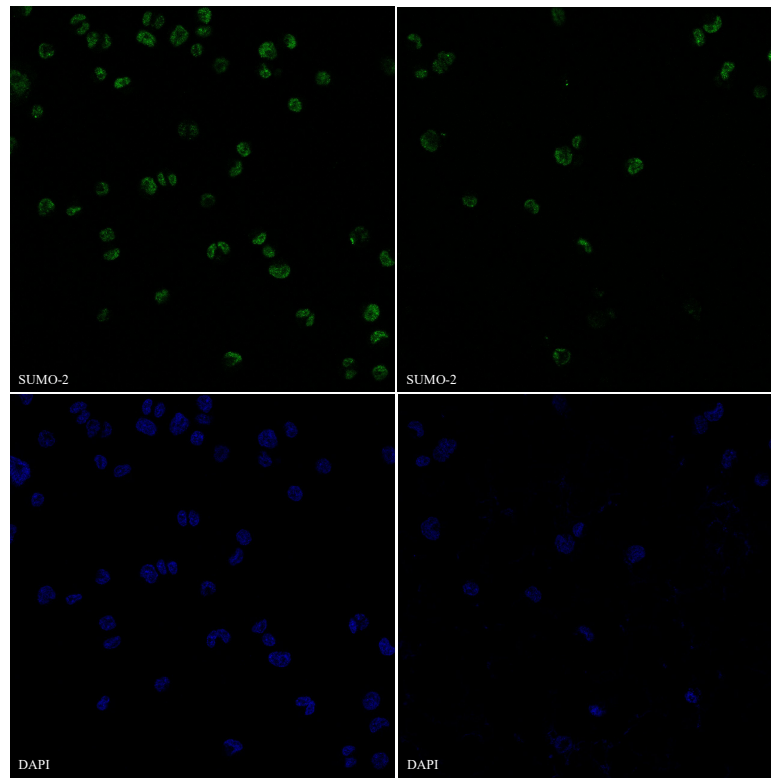


Figure 6.11. SUMO-2 labeling in THP-1 cells. Clockwise starting from upper-left panel: SUMO-2 labeling in non-infected cells, SUMO-2 labeling in infected cells, DAPI labeling in infected cells, DAPI labeling in non-infected cells.

Next, we performed an *in situ* PLA to investigate the presence of SUMO-1 modification on Cas9 in THP-1 cells. For this purpose, we infected THP-1 cells as described above and performed a PLA. Our results failed to show an interaction between Cas9 and SUMO-1 (Figure 6.12). However, the control group where we attempted to visualize Cas9 in the infected cells via immunocytochemistry also failed to show Cas9 labeling. As such, we were unable to draw any conclusions regarding whether Cas9 may actually get sumoylated in our system, although the lack of Cas9 labeling may imply scarce presence of this protein in the eukaryotic environment, rendering it practically inaccessible to the SUMO machinery.

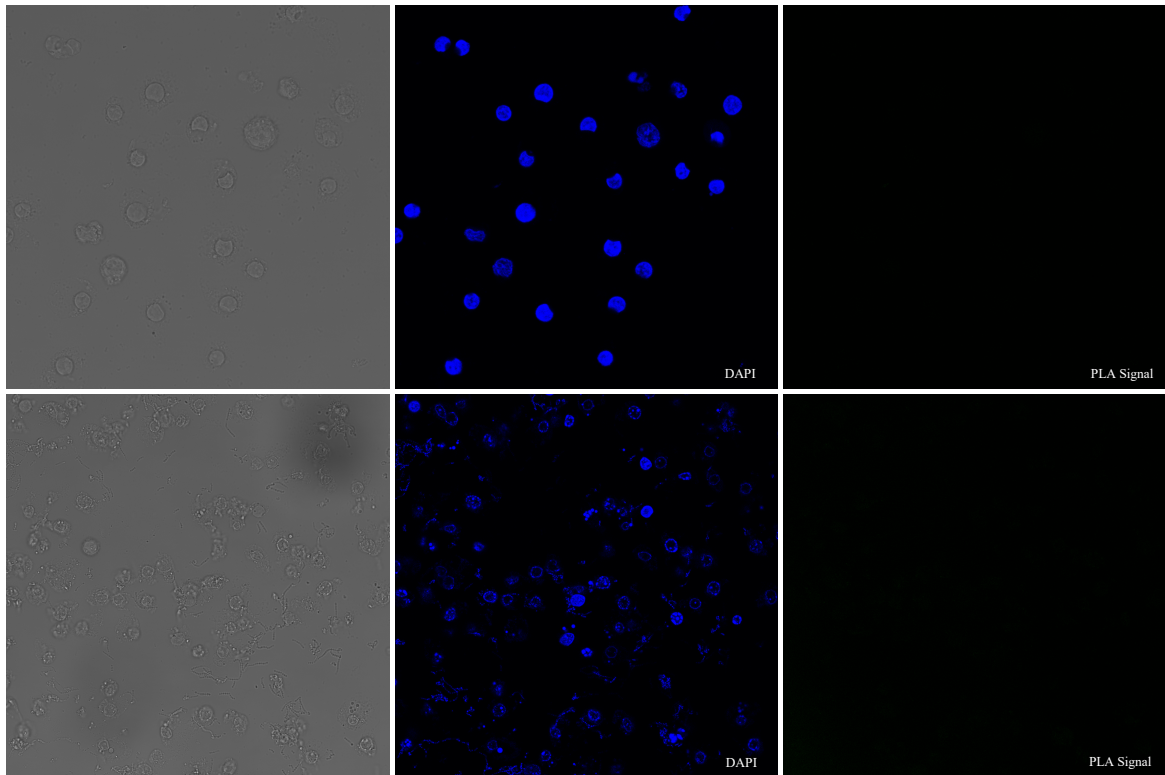


Figure 6.12. Proximity ligation assay for SUMO-1-Cas9 interaction. Top row: non-infected THP-1 cells. Bottom row: infected THP-1 cells. From left to right: bright field, DAPI, and PLA signal.

7. DISCUSSION

7.1. Ubiquitylation of Cas9

In this project, we investigated the eukaryotic post-translational modifications on Cas9 protein, with the hopes of gaining an insight into how this bacterial protein might be regulated in human cells and what the implications of such regulation might be for CRISPR-based applications. Our results from multiple experimental approaches showed for the first time that Cas9 is subject to ubiquitylation in human cell lines, which seems to be decreasing the stability of the modified protein via proteasomal degradation (Figures 6.2, 6.3, 6.4, 6.5). We were able to verify our findings in Cas9-stable cell lines, which constitute a more relevant system for the current CRISPR-based applications. These results are in line with the previous findings by another group which showed that fusing a ubiquitin protein to Cas9 leads to decreased half-life in non-human primate embryos, leading to reduced mosaicism (Tu *et al.*, 2017). Our PLA results in Cas9-inducible HK-2 cells show that Cas9 is heavily ubiquitylated with endogenous levels of this modifier.

We pursued our line of investigation by pinpointing the specific sites on SpCas9 that get ubiquitylated, which according to our preliminary mass spectrometry data seem to be spanning over 11 Lys residues. A better understanding of how the ubiquitin-proteasome system regulates wild-type Cas9 in human cells could help us fine-tune the stability of this important protein for different applications. While our mass spectrometry results give us all the ubiquitin-modified Lys residues, future quantitative proteomic analyses (e.g. SILAC) could tell us which residues qualify as major ubiquitylation sites. As a follow-up, these major ubiquitylation sites will be mutated into arginine, thus precluding modification. Generation of the relevant mutant constructs will help us explore the functional consequences of Cas9 ubiquitylation in greater detail, which may include alterations in the on and off rates for DNA binding, target specificity, and enzymatic efficiency aside from stability.

Moreover, ubiquitylation of Cas9 may also constitute an evolutionarily conserved intracellular response mechanism against microbial invasion. Polyubiquitin chains were

previously shown to coat the extracellular membrane surface of *Salmonella enterica*, an intracellular bacterium, and this modification was shown to be among the prerequisite steps leading to autophagy response following infection (Wang *et al.*, 2018). Similarly, ubiquitylation of Cas9 may play a part in innate immunity against the invading pathogen. Another possibility is that the ubiquitylation of Cas9 in eukaryotes is purely incidental and may reflect an analogous modification of this enzyme by the prokaryotic ubiquitin-like protein (Pup) in bacteria. Nevertheless, ubiquitin modification does seem to have functional consequences for Cas9, as our data suggest that proteasomal degradation may be at play.

7.2. Sumoylation of Cas9 in the Infection System

Our laboratory previously showed that overexpressed or stably-expressed Cas9 gets sumoylated (unpublished data). A part of this project involved the demonstration of Cas9 sumoylation in a natural setting whereby we attempted to simulate *S. pyogenes* infection of human cells. While this bacterium usually colonizes the epithelial cell surfaces, an accumulating body of evidence suggests that *S. pyogenes* can also invade human cells as an intracellular pathogen (Rohde and Cleary, 2016). However, the invasive capabilities of *S. pyogenes* in cell culture seem to be contingent upon sufficient cell surface expression levels of the fibronectin-binding SfbI and F protein, and other proteins also modulate the invasiveness phenotype (Molinari *et al.*, 1997; Okada *et al.*, 1998). Our attempts to infect the epithelium-derived HeLa and HK-2 cells with a patient-derived M2 strain of *S. pyogenes* were unsuccessful, potentially due to the non-compatible state of our particular clinical isolate. For instance, the SfbI protein is only expressed in 70% percent of clinical isolates (Valentin-Weigand *et al.*, 1994). As the genotype of the isolate we used is unclear, future experiments would benefit from obtaining multiple isolates and selecting them for invasiveness.

After infecting the THP-1 cells with *S. pyogenes*, we proceeded with the immunocytochemical labeling of Cas9 and SUMO proteins. Although SUMO isoforms were stained successfully in both infected and non-infected cells, we were unable to consistently detect Cas9 presence in the infected cells. There are several explanations for this outcome. One potential issue could be inadequate internalization of bacteria by our THP-1 cells, which might be inferred given the low number of colony forming units we observed after lysing

the cells and spreading the lysate on blood agar plates. However, a confounding factor is the bactericidal activity of THP-1 cells which might also account for the low survival rates of internalized bacteria (Raza *et al.*, 2000). Moreover, z-stack confocal images also revealed prevalent internalization of *S. pyogenes* by THP-1.

One other explanation for the lack of staining is that Cas9 is not present in the eukaryotic cytosol following infection and, as such, not accessible to our antibodies. If sumoylation of Cas9 is an evolutionarily-conserved natural process, we would expect Cas9 to be found as a soluble protein within the eukaryotic cell to interact with the host SUMO machinery. Nevertheless, to date, there are no reports of Cas9 surviving or operating naturally in eukaryotic cells. If this process indeed occurs as part of host-pathogen interactions, it might rely on specialized bacterial secretion systems which serve to enhance virulence by delivering molecular components that disrupt host defense systems into eukaryotic cells (Zhang *et al.*, 2012). If this is the case, internalization of bacteria might not be a necessary precursor for the existence of Cas9 in the host cytoplasm. Alternatively, Cas9 might get released and exposed to the SUMO machinery following internalization and destruction of bacteria. We were able to visualize Cas9 through immunocytochemical staining, albeit sparsely, which suggests that either of these two processes might be at play. Nevertheless, it is also unclear how the staining protocol might be optimized to yield better results, as the exact conditions that are conducive to Cas9 release are unknown, and it is possible that Cas9 release and sumoylation are time-dependent events. In any case, we were unable to detect any PLA signals representing Cas9 sumoylation, which is expected given the lack of Cas9 labeling. Consequently, we are unable to reach any conclusions as to whether Cas9 sumoylation, which we have discovered in our laboratory under overexpression conditions, is a natural process.

Although we have not been able to demonstrate that ubiquitylation or sumoylation of Cas9 occurs in nature, our findings in cell culture-based experiments are highly relevant for CRISPR applications. As detailed in the introduction of this thesis, PTMs may modulate a protein's interactome, half-life, activity or localization. Moreover, several Cas9 SUMO motifs are found within the nt-groove, which stabilizes interactions with the non-target strand of the target DNA sequence (Slaymaker *et al.*, 2016). Mutating the positively-charged residues within this groove into neutral amino acids resulted in significantly less off-target

binding events (Slaymaker *et al.*, 2016). Incidentally, several of these mutated sites correspond to canonical SUMO motifs, and one of these, K848, led to significantly increased specificity in Cas9 activity (Slaymaker *et al.*, 2016). It is possible that the abolishment of SUMO modification on this site is a contributing factor to the functional modification of this protein. Duygu Yesildag from our group has generated the lysine-to-arginine mutants for all candidate sumoylation sites, and after mass spectrometry analysis to determine which residues are *bona fide* sumoylation sites, we aim to move on to functional assays that will help us parse out the specific effects of each mutation with regards to diverse outcomes such as off-target effects and stability.

To our knowledge, our group has defined the first two eukaryotic PTMs on the prokaryotic Cas9 protein. Both SUMO and ubiquitin modifications are known to be highly sensitive to infection status, and several pathogens are known to interfere with these processes through protease effectors that reverse these PTMs (Ribet and Cossart, 2010). Given the importance of these modifications in host-pathogen interactions and the downregulation of global sumoylation by pathogens such as *Listeria monocytogenes*, it is likely that many other bacterial proteins also get sumoylated as part of a host defense mechanism (Ribet and Cossart, 2010). Conversely, Anaplasmatataceae family members were found to recruit host SUMOylation machinery to actively induce the sumoylation of their own proteins. Similarly, the *Anaplasma phagocytophilum* protein AmpA and *Ehrlichia chaffeensis* protein TRP120 were found to be modified by SUMO isoforms after infection or overexpression in eukaryotic cells (Dunphy *et al.*, 2014; Beyer *et al.*, 2015). Curiously, both of these proteins are injected into the host cell cytoplasm via secretion systems.

To summarize, we have discovered that stably-expressed Cas9 protein gets ubiquitylated in eukaryotic cells, and we were unable to detect sumoylation of the endogenous Cas9 protein following infection of a human monocytic cell line. An improved understanding of the eukaryotic post-translational regulation of Cas9 would help paint a clearer picture of host-pathogen interaction mechanisms, while potentially revealing previously unknown roles of Cas9 in eukaryotic cells. We aim to contribute to this understanding through future work focusing on the practical consequences of Cas9 sumoylation and ubiquitylation.

REFERENCES

- Ahmad, H. I., Ahmad, M. J., Asif, A. R., Adnan, M., Iqbal, M. K., Mehmood, K., ... Xie, S. (2018). A review of crispr-based genome editing: Survival, evolution and challenges. *Current Issues in Molecular Biology*. <https://doi.org/10.21775/cimb.028.047>
- Anders, C., Niewoehner, O., Duerst, A., & Jinek, M. (2014). Structural basis of PAM-dependent target DNA recognition by the Cas9 endonuclease. *Nature*, *513*(7519), 569–573. <https://doi.org/10.1038/nature13579>
- Baliou, S., Adamaki, M., Kyriakopoulos, A. M., Spandidos, D. A., Panayiotidis, M., Christodoulou, I., & Zoumpourlis, V. (2018). CRISPR therapeutic tools for complex genetic disorders and cancer (Review). *International Journal of Oncology*, *53*(2), 443–468. <https://doi.org/10.3892/ijo.2018.4434>
- Barrangou, R., Fremaux, C., Deveau, H., Richards, M., Boyaval, P., Moineau, S., ... Horvath, P. (2007). CRISPR provides acquired resistance against viruses in prokaryotes. *Science*. <https://doi.org/10.1126/science.1138140>
- Baum, C. (2007). Insertional mutagenesis in gene therapy and stem cell biology. *Current Opinion in Hematology*. <https://doi.org/10.1097/MOH.0b013e3281900f01>
- Beyer, A. R., Truchan, H. K., May, L. J., Walker, N. J., Borjesson, D. L., & Carlyon, J. A. (2015). The *Anaplasma phagocytophilum* effector AmpA hijacks host cell SUMOylation. *Cellular Microbiology*, *17*(4), 504–519. <https://doi.org/10.1111/cmi.12380>
- Bibikova, M., Golic, M., Golic, K. G., & Carroll, D. (2002). Targeted chromosomal cleavage and mutagenesis in *Drosophila* using zinc-finger nucleases. *Genetics*. <https://doi.org/10.1126/science.287.5461.2185>
- Blaese, R. M., Culver, K. W., Miller, A. D., Carter, C. S., Fleisher, T., Clerici, M., ... Anderson, W. F. (1995). T lymphocyte-directed gene therapy for ADA-SCID: Initial trial results after 4 years. *Science*. <https://doi.org/10.1126/science.270.5235.475>

- Bolotin, A., Quinquis, B., Sorokin, A., & Dusko Ehrlich, S. (2005). Clustered regularly interspaced short palindrome repeats (CRISPRs) have spacers of extrachromosomal origin. *Microbiology*. <https://doi.org/10.1099/mic.0.28048-0>
- Brouns, S. J. J., Jore, M. M., Lundgren, M., Westra, E. R., Slijkhuis, R. J. H., Snijders, A. P. L., ... van der Oost, J. (2008). Small CRISPR RNAs Guide Antiviral Defense in Prokaryotes. *Science*, *321*(5891), 960–964. <https://doi.org/10.1126/science.1159689>
- Cain, J. A., Solis, N., & Cordwell, S. J. (2014). Beyond gene expression: The impact of protein post-translational modifications in bacteria. *Journal of Proteomics*, *97*, 265–286. <https://doi.org/10.1016/j.jprot.2013.08.012>
- Carroll, D. (2008). Progress and prospects: Zinc-finger nucleases as gene therapy agents. *Gene Therapy*. <https://doi.org/10.1038/gt.2008.145>
- Cavazzana-Calvo, M., Hacein-Bey, S., de Saint Basile, G., Gross, F., Yvon, E., Nusbaum, P., ... Fischer, A. (2000). Gene therapy of human severe combined immunodeficiency (SCID)-X1 disease. *Science (New York, N.Y.)*, *288*(5466), 669–672. Retrieved from <http://www.ncbi.nlm.nih.gov/pubmed/10784449>
- Charlesworth, C. T., Deshpande, P. S., Dever, D. P., Dejene, B., Gomez-Ospina, N., Mantri, S., ... Porteus, M. H. (2018). Identification of Pre-Existing Adaptive Immunity to Cas9 Proteins in Humans. *BioRxiv*, 243345. <https://doi.org/10.1101/243345>
- Chau, V., Tobias, J. W., Bachmair, A., Marriott, D., Ecker, D. J., Gonda, D. K., & Varshavsky, A. (1989). A multiubiquitin chain is confined to specific lysine in a targeted short-lived protein. *Science (New York, N.Y.)*, *243*(4898), 1576–1583. Retrieved from <http://www.ncbi.nlm.nih.gov/pubmed/2538923>
- Chen, Z. J., & Sun, L. J. (2009). Nonproteolytic Functions of Ubiquitin in Cell Signaling. *Molecular Cell*, *33*(3), 275–286. <https://doi.org/10.1016/j.molcel.2009.01.014>
- Choulika, A., Perrin, A., Dujon, B., & Nicolas, J. F. (1995). Induction of homologous recombination in mammalian chromosomes by using the I-SceI system of *Saccharomyces cerevisiae*. *Molecular and Cellular Biology*, *15*(4), 1968–1973. Retrieved from <http://www.ncbi.nlm.nih.gov/pubmed/7891691>

- Cong, L., Ran, F. A., Cox, D., Lin, S., Barretto, R., Habib, N., ... Zhang, F. (2013). Multiplex genome engineering using CRISPR/Cas systems. *Science (New York, N.Y.)*, 339(6121), 819–823. <https://doi.org/10.1126/science.1231143>
- Cristalli, G., Costanzi, S., Lambertucci, C., Lupidi, G., Vittori, S., Volpini, R., & Camaioni, E. (2001). Adenosine deaminase: Functional implications and different classes of inhibitors. *Medicinal Research Reviews*. [https://doi.org/10.1002/1098-1128\(200103\)21:2<105::AID-MED1002>3.0.CO;2-U](https://doi.org/10.1002/1098-1128(200103)21:2<105::AID-MED1002>3.0.CO;2-U)
- Cyranoski, D., & Ledford, H. (2018). Genome-edited baby claim provokes international outcry. *Nature*, 563(7733), 607–608. <https://doi.org/10.1038/d41586-018-07545-0>
- Davis, K. M., Pattanayak, V., Thompson, D. B., Zuris, J. A., & Liu, D. R. (2015). Small molecule-triggered Cas9 protein with improved genome-editing specificity. *Nature Chemical Biology*, 11(5), 316–318. <https://doi.org/10.1038/nchembio.1793>
- Deltcheva, E., Chylinski, K., Sharma, C. M., Gonzales, K., Chao, Y., Pirzada, Z. A., ... Charpentier, E. (2011). CRISPR RNA maturation by trans-encoded small RNA and host factor RNase III. *Nature*, 471(7340), 602–607. <https://doi.org/10.1038/nature09886>
- Desterro, J. M. P., Rodriguez, M. S., & Hay, R. T. (1998). SUMO-1 Modification of IB Inhibits NF-B Activation. *Molecular Cell* (Vol. 2). Retrieved from <https://www.sciencedirect.com/science/article/pii/S1097276500801331>
- Deveau, H., Barrangou, R., Garneau, J. E., Labonte, J., Fremaux, C., Boyaval, P., ... Moineau, S. (2008). Phage Response to CRISPR-Encoded Resistance in *Streptococcus thermophilus*. *Journal of Bacteriology*, 190(4), 1390–1400. <https://doi.org/10.1128/JB.01412-07>
- Doudna, J. A., & Charpentier, E. (2014). The new frontier of genome engineering with CRISPR-Cas9. *Science*. <https://doi.org/10.1126/science.1258096>
- Duan, G., & Walther, D. (2015). The Roles of Post-translational Modifications in the Context of Protein Interaction Networks. *PLOS Computational Biology*, 11(2), e1004049. <https://doi.org/10.1371/journal.pcbi.1004049>

- Dunbar, C. E., High, K. A., Joung, J. K., Kohn, D. B., Ozawa, K., & Sadelain, M. (2018). Gene therapy comes of age. *Science*. <https://doi.org/10.1126/science.aan4672>
- Dunphy, P. S., Luo, T., & McBride, J. W. (2014). Ehrlichia chaffeensis exploits host SUMOylation pathways to mediate effector-host interactions and promote intracellular survival. *Infection and Immunity*, 82(10), 4154–4168. <https://doi.org/10.1128/IAI.01984-14>
- Engel, B. J., Bowser, J. L., Broaddus, R. R., & Carson, D. D. (2016). MUC1 stimulates EGFR expression and function in endometrial cancer. *Oncotarget*, 7(22), 32796–32809. <https://doi.org/10.18632/oncotarget.8743>
- Firth, A. L., Menon, T., Parker, G. S., Qualls, S. J., Lewis, B. M., Ke, E., ... Verma, I. M. (2015). Functional Gene Correction for Cystic Fibrosis in Lung Epithelial Cells Generated from Patient iPSCs. *Cell Reports*, 12(9), 1385–1390. <https://doi.org/10.1016/j.celrep.2015.07.062>
- Flotho, A., & Melchior, F. (2013). Sumoylation: A Regulatory Protein Modification in Health and Disease. *Annual Review of Biochemistry*, 82(1), 357–385. <https://doi.org/10.1146/annurev-biochem-061909-093311>
- Garneau, J. E., Dupuis, M.-È., Villion, M., Romero, D. A., Barrangou, R., Boyaval, P., ... Moineau, S. (2010). The CRISPR/Cas bacterial immune system cleaves bacteriophage and plasmid DNA. *Nature*, 468(7320), 67–71. <https://doi.org/10.1038/nature09523>
- Gasiunas, G., Barrangou, R., Horvath, P., & Siksnys, V. (2012). Cas9-crRNA ribonucleoprotein complex mediates specific DNA cleavage for adaptive immunity in bacteria. *Proceedings of the National Academy of Sciences*, 109(39), E2579–E2586. <https://doi.org/10.1073/pnas.1208507109>
- Gaudelli, N. M., Komor, A. C., Rees, H. A., Packer, M. S., Badran, A. H., Bryson, D. I., & Liu, D. R. (2017). Programmable base editing of A•T to G•C in genomic DNA without DNA cleavage. *Nature*, 551(7681), 464–471. <https://doi.org/10.1038/nature24644>
- Geiss-Friedlander, R., & Melchior, F. (2007). Concepts in sumoylation: a decade on. *Nature Reviews Molecular Cell Biology*, 8(12), 947–956. <https://doi.org/10.1038/nrm2293>

- Greco, R., De Martino, L., Donnarumma, G., Conte, M., Seganti, L., & Valenti, P. (1995). Invasion of cultured human cells by *Streptococcus pyogenes*. *Research in Microbiology*, *146*(7), 551–560. [https://doi.org/10.1016/0923-2508\(96\)80561-4](https://doi.org/10.1016/0923-2508(96)80561-4)
- Guha, T. K., Wai, A., & Hausner, G. (2017). Programmable Genome Editing Tools and their Regulation for Efficient Genome Engineering. *Computational and Structural Biotechnology Journal*. <https://doi.org/10.1016/j.csbj.2016.12.006>
- Gutschner, T., Haemmerle, M., Genovese, G., Draetta, G. F., & Chin, L. (2016). Post-translational Regulation of Cas9 during G1 Enhances Homology-Directed Repair. *Cell Reports*, *14*(6), 1555–1566. <https://doi.org/10.1016/j.celrep.2016.01.019>
- Haapaniemi, E., Botla, S., Persson, J., Schmierer, B., & Taipale, J. (2018). CRISPR-Cas9 genome editing induces a p53-mediated DNA damage response. *Nature Medicine*. <https://doi.org/10.1038/s41591-018-0049-z>
- Haas, A. L., Warms, J. V, Hershko, A., & Rose, I. A. (1982). Ubiquitin-activating enzyme. Mechanism and role in protein-ubiquitin conjugation. *The Journal of Biological Chemistry*, *257*(5), 2543–2548. Retrieved from <http://www.ncbi.nlm.nih.gov/pubmed/6277905>
- Hacein-Bey-Abina, S., Von Kalle, C., Schmidt, M., McCormack, M. P., Wulffraat, N., Leboulch, P., ... Cavazzana-Calvo, M. (2003). LMO2-Associated Clonal T Cell Proliferation in Two Patients after Gene Therapy for SCID-X1. *Science*. <https://doi.org/10.1126/science.1088547>
- Hay, R. T. (2005). Review SUMO: A History of Modification. *Molecular Cell*, *18*, 1–12. <https://doi.org/10.1016/j.molcel.2005.03.012>
- Hayashi, M., Saito, Y., & Kawashima, S. (1992). Calpain activation is essential for membrane fusion of erythrocytes in the presence of exogenous Ca²⁺. *Biochemical and Biophysical Research Communications*, *182*(2), 939–946. Retrieved from <http://www.ncbi.nlm.nih.gov/pubmed/1734892>
- Hendriks, I. A., & Vertegaal, A. C. O. (2016). A comprehensive compilation of SUMO proteomics. *Nature Reviews Molecular Cell Biology*, *17*(9), 581–595. <https://doi.org/10.1038/nrm.2016.81>

- Heyer, W.-D., Ehmsen, K. T., & Liu, J. (2010). Regulation of homologous recombination in eukaryotes. *Annual Review of Genetics*, *44*, 113–139. <https://doi.org/10.1146/annurev-genet-051710-150955>
- Hickey, C. M., Wilson, N. R., & Hochstrasser, M. (2012). Function and regulation of SUMO proteases. *Nature Reviews Molecular Cell Biology*, *13*(12), 755–766. <https://doi.org/10.1038/nrm3478>
- Hochstrasser, M. (1996). Ubiquitin-Dependent Protein Degradation. *Annual Review of Genetics*, *30*(1), 405–439. <https://doi.org/10.1146/annurev.genet.30.1.405>
- Howden, S. E., McColl, B., Glaser, A., Vadolas, J., Petrou, S., Little, M. H., ... Stanley, E. G. (2016). A Cas9 Variant for Efficient Generation of Indel-Free Knockin or Gene-Corrected Human Pluripotent Stem Cells. *Stem Cell Reports*, *7*(3), 508–517. <https://doi.org/10.1016/j.stemcr.2016.07.001>
- Hsu, P. D., Scott, D. A., Weinstein, J. A., Ran, F. A., Konermann, S., Agarwala, V., ... Zhang, F. (2013). DNA targeting specificity of RNA-guided Cas9 nucleases. *Nature Biotechnology*, *31*(9), 827–832. <https://doi.org/10.1038/nbt.2647>
- Hsu, P. D., Lander, E. S., & Zhang, F. (2014). Development and applications of CRISPR-Cas9 for genome engineering. *Cell*. <https://doi.org/10.1016/j.cell.2014.05.010>
- Ishino, Y., Shinagawa, H., Makino, K., Amemura, M., & Nakamura, A. (1987). Nucleotide sequence of the *iap* gene, responsible for alkaline phosphatase isoenzyme conversion in *Escherichia coli*, and identification of the gene product. *Journal of Bacteriology*. <https://doi.org/10.1128/jb.169.12.5429-5433.1987>
- Jansen, R., Van Embden, J. D. A., Gaastra, W., & Schouls, L. M. (2002). Identification of genes that are associated with DNA repeats in prokaryotes. *Molecular Microbiology*. <https://doi.org/10.1046/j.1365-2958.2002.02839.x>
- Jasin, M. (1996). Genetic manipulation of genomes with rare-cutting endonucleases. *Trends in Genetics*. [https://doi.org/10.1016/0168-9525\(96\)10019-6](https://doi.org/10.1016/0168-9525(96)10019-6)
- Jeggo, P. A. (1998). 5 DNA Breakage and Repair. *Advances in Genetics*. [https://doi.org/10.1016/S0065-2660\(08\)60144-3](https://doi.org/10.1016/S0065-2660(08)60144-3)

- Jiang, F., Zhou, K., Ma, L., Gressel, S., & Doudna, J. A. (2015). STRUCTURAL BIOLOGY. A Cas9-guide RNA complex preorganized for target DNA recognition. *Science (New York, N.Y.)*, *348*(6242), 1477–1481. <https://doi.org/10.1126/science.aab1452>
- Jinek, M., Chylinski, K., Fonfara, I., Hauer, M., Doudna, J. A., & Charpentier, E. (2012). A Programmable Dual-RNA-Guided DNA Endonuclease in Adaptive Bacterial Immunity. *Science*, *337*(6096), 816–821. <https://doi.org/10.1126/science.1225829>
- Jinek, M., Jiang, F., Taylor, D. W., Sternberg, S. H., Kaya, E., Ma, E., ... Doudna, J. A. (2014). Structures of Cas9 Endonucleases Reveal RNA-Mediated Conformational Activation. *Science*, *343*(6176), 1247997–1247997. <https://doi.org/10.1126/science.1247997>
- Jürgen Dohmen, R. (2004). SUMO protein modification. *Biochimica et Biophysica Acta (BBA) - Molecular Cell Research*, *1695*(1–3), 113–131. <https://doi.org/10.1016/J.BBAMCR.2004.09.021>
- Kavlashvili, T., Jia, Y., Dai, D., Meng, X., Thiel, K. W., Leslie, K. K., & Yang, S. (2016). Inverse Relationship between Progesterone Receptor and Myc in Endometrial Cancer. *PloS One*, *11*(2), e0148912. <https://doi.org/10.1371/journal.pone.0148912>
- Kawamura, N., Nimura, K., Nagano, H., Yamaguchi, S., Nonomura, N., & Kaneda, Y. (2015). CRISPR/Cas9-mediated gene knockout of NANOG and NANOGP8 decreases the malignant potential of prostate cancer cells. *Oncotarget*, *6*(26), 22361–22374. <https://doi.org/10.18632/oncotarget.4293>
- Komander, D., Clague, M. J., & Urbé, S. (2009). Breaking the chains: structure and function of the deubiquitinases. *Nature Reviews Molecular Cell Biology*, *10*(8), 550–563. <https://doi.org/10.1038/nrm2731>
- Komor, A. C., Kim, Y. B., Packer, M. S., Zuris, J. A., & Liu, D. R. (2016). Programmable editing of a target base in genomic DNA without double-stranded DNA cleavage. *Nature*, *533*(7603), 420–424. <https://doi.org/10.1038/nature17946>

- Kosicki, M., Tomberg, K., & Bradley, A. (2018). Repair of double-strand breaks induced by CRISPR–Cas9 leads to large deletions and complex rearrangements. *Nature Biotechnology*, 36(8), 765. <https://doi.org/10.1038/nbt.4192>
- Leenay, R. T., Maksimchuk, K. R., Slotkowski, R. A., Agrawal, R. N., Gomaa, A. A., Briner, A. E., ... Beisel, C. L. (2016). Identifying and Visualizing Functional PAM Diversity across CRISPR-Cas Systems. *Molecular Cell*. <https://doi.org/10.1016/j.molcel.2016.02.031>
- Li, G., Zhang, X., Zhong, C., Mo, J., Quan, R., Yang, J., ... Wu, Z. (2017). Small molecules enhance CRISPR/Cas9-mediated homology-directed genome editing in primary cells. *Scientific Reports*, 7(1), 8943. <https://doi.org/10.1038/s41598-017-09306-x>
- Li, P., Kleinstiver, B. P., Leon, M. Y., Prew, M. S., Navarro-Gomez, D., Greenwald, S. H., ... Liu, Q. (2018). Allele-Specific CRISPR-Cas9 Genome Editing of the Single-Base P23H Mutation for Rhodopsin-Associated Dominant Retinitis Pigmentosa. *The CRISPR Journal*. <https://doi.org/10.1089/crispr.2017.0009>
- Li, T., Huang, S., Jiang, W. Z., Wright, D., Spalding, M. H., Weeks, D. P., & Yang, B. (2011). TAL nucleases (TALNs): hybrid proteins composed of TAL effectors and FokI DNA-cleavage domain. *Nucleic Acids Research*, 39(1), 359–372. <https://doi.org/10.1093/nar/gkq704>
- Liang, P., Xu, Y., Zhang, X., Ding, C., Huang, R., Zhang, Z., ... Huang, J. (2015). CRISPR/Cas9-mediated gene editing in human tripronuclear zygotes. *Protein & Cell*, 6(5), 363–372. <https://doi.org/10.1007/s13238-015-0153-5>
- Lundstrom, K. (2018). Viral Vectors in Gene Therapy. *Diseases*, 6(2), 42. <https://doi.org/10.3390/diseases6020042>
- Ma, H., Marti-Gutierrez, N., Park, S.-W., Wu, J., Lee, Y., Suzuki, K., ... Mitalipov, S. (2017). Correction of a pathogenic gene mutation in human embryos. *Nature*, 548(7668), 413–419. <https://doi.org/10.1038/nature23305>

- Maeder, M. L., Linder, S. J., Cascio, V. M., Fu, Y., Ho, Q. H., & Joung, J. K. (2013). CRISPR RNA-guided activation of endogenous human genes. *Nature Methods*, *10*(10), 977–979. <https://doi.org/10.1038/nmeth.2598>
- Makarova, K. S., Wolf, Y. I., Alkhnbashi, O. S., Costa, F., Shah, S. A., Saunders, S. J., ... Koonin, E. V. (2015). An updated evolutionary classification of CRISPR–Cas systems. *Nature Reviews Microbiology*, *13*(11), 722–736. <https://doi.org/10.1038/nrmicro3569>
- Makarova, K. S., Zhang, F., & Koonin, E. V. (2017). SnapShot: Class 2 CRISPR-Cas Systems. *Cell*, *168*(1–2), 328–328.e1. <https://doi.org/10.1016/j.cell.2016.12.038>
- Mali, P., Esvelt, K. M., & Church, G. M. (2013). Cas9 as a versatile tool for engineering biology. *Nature Methods*. <https://doi.org/10.1038/nmeth.2649>
- Mansoori, B., Shotorbani, S. S., & Baradaran, B. (2014). RNA interference and its role in cancer therapy. *Advanced Pharmaceutical Bulletin*. <https://doi.org/10.5681/apb.2014.046>
- Mao, Z., Bozzella, M., Seluanov, A., & Gorbunova, V. (2008). Comparison of nonhomologous end joining and homologous recombination in human cells. *DNA Repair*, *7*(10), 1765–1771. <https://doi.org/10.1016/j.dnarep.2008.06.018>
- Martin, S., Wilkinson, K. A., Nishimune, A., & Henley, J. M. (2007). Emerging extranuclear roles of protein SUMOylation in neuronal function and dysfunction. *Nature Reviews Neuroscience*, *8*(12), 948–959. <https://doi.org/10.1038/nrn2276>
- Maruyama, T., Dougan, S. K., Truttmann, M. C., Bilate, A. M., Ingram, J. R., & Ploegh, H. L. (2015). Increasing the efficiency of precise genome editing with CRISPR-Cas9 by inhibition of nonhomologous end joining. *Nature Biotechnology*, *33*(5), 538–542. <https://doi.org/10.1038/nbt.3190>
- McDonald, J. I., Celik, H., Rois, L. E., Fishberger, G., Fowler, T., Rees, R., ... Challen, G. A. (2016). Reprogrammable CRISPR/Cas9-based system for inducing site-specific DNA methylation. *Biology Open*, *5*(6), 866–874. <https://doi.org/10.1242/bio.019067>

- Mehravar, M., Shirazi, A., Nazari, M., & Banan, M. (2018). Mosaicism in CRISPR/Cas9-mediated genome editing. *Developmental Biology*. <https://doi.org/10.1016/J.YDBIO.2018.10.008>
- Meyer, H. J., & Rape, M. (2014). Enhanced protein degradation by branched ubiquitin chains. *Cell*, *157*(4), 910–921. <https://doi.org/10.1016/j.cell.2014.03.037>
- Miller, J. C., Tan, S., Qiao, G., Barlow, K. A., Wang, J., Xia, D. F., ... Rebar, E. J. (2011). A TALE nuclease architecture for efficient genome editing. *Nature Biotechnology*. <https://doi.org/10.1038/nbt.1755>
- Mo, O. (2015). CRISPR-Cas9 Human Genome Editing: Challenges, Ethical Concerns and Implications. *Journal of Clinical Research & Bioethics*, *06*(06), 1–3. <https://doi.org/10.4172/2155-9627.1000253>
- Mojica, F. J. M., Díez-Villaseñor, C., García-Martínez, J., & Soria, E. (2005). Intervening sequences of regularly spaced prokaryotic repeats derive from foreign genetic elements. *Journal of Molecular Evolution*. <https://doi.org/10.1007/s00239-004-0046-3>
- Molinari, G., Talay, S. R., Valentin-Weigand, P., Rohde, M., & Chhatwal, G. S. (1997). *The Fibronectin-Binding Protein of Streptococcus pyogenes, SfbI, Is Involved in the Internalization of Group A Streptococci by Epithelial Cells. INFECTION AND IMMUNITY* (Vol. 65). Retrieved from <https://www.ncbi.nlm.nih.gov/pmc/articles/PMC175140/pdf/651357.pdf>
- Müller, S., Matunis, M. J., & Dejean, A. (1998). Conjugation with the ubiquitin-related modifier SUMO-1 regulates the partitioning of PML within the nucleus. *The EMBO Journal*, *17*(1), 61–70. <https://doi.org/10.1093/emboj/17.1.61>
- Nacerddine, K., Lehembre, F., Bhaumik, M., Artus, J., Cohen-Tannoudji, M., Babinet, C., ... Dejean, A. (2005). The SUMO Pathway Is Essential for Nuclear Integrity and Chromosome Segregation in Mice. *Developmental Cell*, *9*(6), 769–779. <https://doi.org/10.1016/j.devcel.2005.10.007>
- Naldini, L. (2015). Gene therapy returns to centre stage. *Nature*, *526*(7573), 351–360. <https://doi.org/10.1038/nature15818>

- Nishimasu, H., Cong, L., Yan, W. X., Ran, F. A., Zetsche, B., Li, Y., ... Nureki, O. (2015). Crystal Structure of *Staphylococcus aureus* Cas9. *Cell*, *162*(5), 1113–1126. <https://doi.org/10.1016/j.cell.2015.08.007>
- Nishimasu, H., Ran, F. A., Hsu, P. D., Konermann, S., Shehata, S. I., Dohmae, N., ... Nureki, O. (2014). Crystal Structure of Cas9 in Complex with Guide RNA and Target DNA. *Cell*, *156*(5), 935–949. <https://doi.org/10.1016/j.cell.2014.02.001>
- O’Geen, H., Yu, A. S., & Segal, D. J. (2015). How specific is CRISPR/Cas9 really? *Current Opinion in Chemical Biology*, *29*, 72–78. <https://doi.org/10.1016/J.CBPA.2015.10.001>
- Okada, N., Tatsuno, I., Hanski, E., Caparon, M., & Sasakawa, C. (1998). Streptococcus pyogenes protein F promotes invasion of HeLa cells. *Microbiology*, *144*(11), 3079–3086. <https://doi.org/10.1099/00221287-144-11-3079>
- Ormond, K. E., Mortlock, D. P., Scholes, D. T., Bombard, Y., Brody, L. C., Faucett, W. A., ... Young, C. E. (2017). Human Germline Genome Editing. *American Journal of Human Genetics*, *101*(2), 167–176. <https://doi.org/10.1016/j.ajhg.2017.06.012>
- Ostermeier, M. (2005). Engineering allosteric protein switches by domain insertion. *Protein Engineering, Design and Selection*, *18*(8), 359–364. <https://doi.org/10.1093/protein/gzi048>
- Park, C.-Y., Kim, D. H., Son, J. S., Sung, J. J., Lee, J., Bae, S., ... Kim, J.-S. (2015). Functional Correction of Large Factor VIII Gene Chromosomal Inversions in Hemophilia A Patient-Derived iPSCs Using CRISPR-Cas9. *Cell Stem Cell*, *17*(2), 213–220. <https://doi.org/10.1016/j.stem.2015.07.001>
- Pelletier, R., Caron, S., & Puymirat, J. (2006). RNA Based Gene Therapy for Dominantly Inherited Diseases. *Current Gene Therapy*. <https://doi.org/10.2174/156652306775515592>
- Polstein, L. R., Perez-Pinera, P., Kocak, D. D., Vockley, C. M., Bledsoe, P., Song, L., ... Gersbach, C. A. (2015). Genome-wide specificity of DNA binding, gene regulation, and chromatin remodeling by TALE- and CRISPR/Cas9-based transcriptional activators. *Genome Research*, *25*(8), 1158–1169. <https://doi.org/10.1101/gr.179044.114>

- Pourcel, C., Salvignol, G., & Vergnaud, G. (2005). CRISPR elements in *Yersinia pestis* acquire new repeats by preferential uptake of bacteriophage DNA, and provide additional tools for evolutionary studies. *Microbiology*. <https://doi.org/10.1099/mic.0.27437-0>
- Prabakaran, S., Lippens, G., Steen, H., & Gunawardena, J. (2012). Post-translational modification: nature's escape from genetic imprisonment and the basis for dynamic information encoding. *Wiley Interdisciplinary Reviews: Systems Biology and Medicine*, 4(6), 565–583. <https://doi.org/10.1002/wsbm.1185>
- Qi, L. S., Larson, M. H., Gilbert, L. A., Doudna, J. A., Weissman, J. S., Arkin, A. P., & Lim, W. A. (2013). Repurposing CRISPR as an RNA-guided platform for sequence-specific control of gene expression. *Cell*, 152(5), 1173–1183. <https://doi.org/10.1016/j.cell.2013.02.022>
- Rape, M. (2017). Ubiquitylation at the crossroads of development and disease. *Nature Reviews Molecular Cell Biology*, 19(1), 59–70. <https://doi.org/10.1038/nrm.2017.83>
- Ravikumar, V., Jers, C., & Mijakovic, I. (2015). Elucidating Host-Pathogen Interactions Based on Post-Translational Modifications Using Proteomics Approaches. *Frontiers in Microbiology*, 6, 1313. <https://doi.org/10.3389/fmicb.2015.01312>
- Raza, M. W., Blackwell, C. C., Elton, R. A., & Weir, D. M. (2000). Bactericidal activity of a monocytic cell line (THP-1) against common respiratory tract bacterial pathogens is depressed after infection with respiratory syncytial virus. *Journal of Medical Microbiology*, 49(3), 227–233. <https://doi.org/10.1099/0022-1317-49-3-227>
- Raza, U., Saatci, Ö., Uhlmann, S., Ansari, S. A., Eyüpoğlu, E., Yurdusev, E., ... Şahin, Ö. (2016). The miR-644a/CTBP1/p53 axis suppresses drug resistance by simultaneous inhibition of cell survival and epithelial-mesenchymal transition in breast cancer. *Oncotarget*, 7(31), 49859–49877. <https://doi.org/10.18632/oncotarget.10489>
- Ribet, D., & Cossart, P. (2010). SUMOylation and bacterial pathogens. *Virulence*, 1:6, 532–534. <https://doi.org/10.4161/viru.1.6.13449>
- Rogers, S., & Pfuderer, P. (1968). Use of viruses as carriers of added genetic information [33]. *Nature*. <https://doi.org/10.1038/219749a0>

- Rohde, M., & Cleary, P. P. (2016). Adhesion and invasion of *Streptococcus pyogenes* into host cells and clinical relevance of intracellular streptococci. *Streptococcus pyogenes : Basic Biology to Clinical Manifestations*. University of Oklahoma Health Sciences Center. Retrieved from <http://www.ncbi.nlm.nih.gov/pubmed/26866223>
- Rouet, P., Smih, F., & Jasin, M. (1994). Introduction of double-strand breaks into the genome of mouse cells by expression of a rare-cutting endonuclease. *Molecular and Cellular Biology*, *14*(12), 8096–8106. Retrieved from <http://www.ncbi.nlm.nih.gov/pubmed/7969147>
- Singh, R., Gupta, S. C., Peng, W.-X., Zhou, N., Pochampally, R., Atfi, A., ... Mo, Y.-Y. (2016). Regulation of alternative splicing of Bcl-x by BC200 contributes to breast cancer pathogenesis. *Cell Death & Disease*, *7*(6), e2262–e2262. <https://doi.org/10.1038/cddis.2016.168>
- Singh, V. K., Kalsan, M., Kumar, N., Saini, A., & Chandra, R. (2015). Induced pluripotent stem cells: applications in regenerative medicine, disease modeling, and drug discovery. *Frontiers in Cell and Developmental Biology*, *3*, 2. <https://doi.org/10.3389/fcell.2015.00002>
- Slymaker, I. M., Gao, L., Zetsche, B., Scott, D. A., Yan, W. X., & Zhang, F. (2016). Rationally engineered Cas9 nucleases with improved specificity. *Science (New York, N.Y.)*, *351*(6268), 84–88. <https://doi.org/10.1126/science.aad5227>
- Starr, T., Bauler, T. J., Malik-Kale, P., & Steele-Mortimer, O. (2018). The phorbol 12-myristate-13-acetate differentiation protocol is critical to the interaction of THP-1 macrophages with *Salmonella Typhimurium*. *PloS One*, *13*(3), e0193601. <https://doi.org/10.1371/journal.pone.0193601>
- Stolberg, S. G. (1999). The biotech death of Jesse Gelsinger. *The New York Times Magazine*, 136–140, 149–150. Retrieved from <http://www.ncbi.nlm.nih.gov/pubmed/11647737>
- Swatek, K. N., & Komander, D. (2016). Ubiquitin modifications. *Cell Research*, *26*(4), 399–422. <https://doi.org/10.1038/cr.2016.39>

- Tatum, E. L. (1966). Molecular biology, nucleic acids, and the future of medicine. *Perspectives in Biology and Medicine*, 10(1), 19–32. Retrieved from <http://www.ncbi.nlm.nih.gov/pubmed/6002665>
- Tsai, S. Q., Wyvekens, N., Khayter, C., Foden, J. A., Thapar, V., Reyon, D., ... Joung, J. K. (2014). Dimeric CRISPR RNA-guided FokI nucleases for highly specific genome editing. *Nature Biotechnology*, 32(6), 569–576. <https://doi.org/10.1038/nbt.2908>
- Tu, Z., Yang, W., Yan, S., Yin, A., Gao, J., Liu, X., ... Li, X.-J. (2017). Promoting Cas9 degradation reduces mosaic mutations in non-human primate embryos. *Scientific Reports*, 7, 42081. <https://doi.org/10.1038/srep42081>
- Urnov, F. D., Rebar, E. J., Holmes, M. C., Zhang, H. S., & Gregory, P. D. (2010). Genome editing with engineered zinc finger nucleases. *Nature Reviews Genetics*. <https://doi.org/10.1038/nrg2842>
- Valentin-Weigand, P., Talay, S. R., Kaufhold, A., Timmis, K. N., & Chhatwal, G. S. (1994). The fibronectin binding domain of the Sfb protein adhesin of *Streptococcus pyogenes* occurs in many group A streptococci and does not cross-react with heart myosin. *Microbial Pathogenesis*, 17(2), 111–120. <https://doi.org/10.1006/mpat.1994.1057>
- Walsh, C. T., Garneau-Tsodikova, S., & Gatto, G. J. (2005). Protein Posttranslational Modifications: The Chemistry of Proteome Diversifications. *Angewandte Chemie International Edition*, 44(45), 7342–7372. <https://doi.org/10.1002/anie.200501023>
- Wang, H., La Russa, M., & Qi, L. S. (2016). CRISPR/Cas9 in Genome Editing and Beyond. *Annual Review of Biochemistry*, 85(1), 227–264. <https://doi.org/10.1146/annurev-biochem-060815-014607>
- Wang, L., Yan, J., Niu, H., Huang, R., & Wu, S. (2018). Autophagy and Ubiquitination in *Salmonella* Infection and the Related Inflammatory Responses. *Frontiers in Cellular and Infection Microbiology*, 8, 78. <https://doi.org/10.3389/fcimb.2018.00078>
- Weisshaar, S. R., Keusekotten, K., Krause, A., Horst, C., Springer, H. M., Götttsche, K., ... Praefcke, G. J. K. (2008). Arsenic trioxide stimulates SUMO-2/3 modification leading to RNF4-dependent proteolytic targeting of PML. *FEBS Letters*, 582(21–22), 3174–3178. <https://doi.org/10.1016/j.febslet.2008.08.008>

- Wimmer, P., Schreiner, S., & Dobner, T. (2012). Human Pathogens and the Host Cell SUMOylation System. *Journal of Virology*, 86(2), 642–654. <https://doi.org/10.1128/JVI.06227-11>
- Xie, F., Ye, L., Chang, J. C., Beyer, A. I., Wang, J., Muench, M. O., & Kan, Y. W. (2014). Seamless gene correction of β -thalassemia mutations in patient-specific iPSCs using CRISPR/Cas9 and piggyBac. *Genome Research*, 24(9), 1526–1533. <https://doi.org/10.1101/gr.173427.114>
- Yang, D., Scavuzzo, M. A., Chmielowiec, J., Sharp, R., Bajic, A., & Borowiak, M. (2016). Enrichment of G2/M cell cycle phase in human pluripotent stem cells enhances HDR-mediated gene repair with customizable endonucleases. *Scientific Reports*, 6, 21264. <https://doi.org/10.1038/srep21264>
- Yen, S.-T., Zhang, M., Deng, J. M., Usman, S. J., Smith, C. N., Parker-Thornburg, J., ... Behringer, R. R. (2014). Somatic mosaicism and allele complexity induced by CRISPR/Cas9 RNA injections in mouse zygotes. *Developmental Biology*, 393(1), 3–9. <https://doi.org/10.1016/J.YDBIO.2014.06.017>
- Yu, C., Liu, Y., Ma, T., Liu, K., Xu, S., Zhang, Y., ... Qi, L. S. (2015). Small molecules enhance CRISPR genome editing in pluripotent stem cells. *Cell Stem Cell*, 16(2), 142–147. <https://doi.org/10.1016/j.stem.2015.01.003>
- Zeng, Y., Li, J., Li, G., Huang, S., Yu, W., Zhang, Y., ... Huang, X. (2018). Correction of the Marfan Syndrome Pathogenic FBN1 Mutation by Base Editing in Human Cells and Heterozygous Embryos. *Molecular Therapy: The Journal of the American Society of Gene Therapy*, 26(11), 2631–2637. <https://doi.org/10.1016/j.ymthe.2018.08.007>
- Zetsche, B., Volz, S. E., & Zhang, F. (2015). A split-Cas9 architecture for inducible genome editing and transcription modulation. *Nature Biotechnology*, 33(2), 139–142. <https://doi.org/10.1038/nbt.3149>
- Zhang, W., Rong, C., Chen, C., & Gao, G. F. (2012). Type-IVC Secretion System: A Novel Subclass of Type IV Secretion System (T4SS) Common Existing in Gram-Positive Genus *Streptococcus*. *PLoS ONE*, 7(10), e46390. <https://doi.org/10.1371/journal.pone.0046390>

- Zhang, X., Choi, P. S., Francis, J. M., Imielinski, M., Watanabe, H., Cherniack, A. D., & Meyerson, M. (2016). Identification of focally amplified lineage-specific super-enhancers in human epithelial cancers. *Nature Genetics*, *48*(2), 176–182. <https://doi.org/10.1038/ng.3470>
- Zinder, N. D., & Lederberg, J. (1952). Genetic exchange in Salmonella. *Journal of Bacteriology*. <https://doi.org/10.1186/s12864-015-1488-2>